UNIVERSITY OF OTTAWA

ATTENUATION OF NEUTRONS BY A LARGE CARBON BLOCK

by

Corrado Glavina

Submitted in Partial Fulfillment
of the Requirements for
The Degree of Master of Science

DEPARTMENT OF PHYSICS
Faculty of Pure and Applied Science
THE UNIVERSITY OF OTTAWA

Ottawa, Canada
April, 1964

ABSTRACT

This experiment is part of a program to study the attenuation of neutrons by large shielding blocks. In this first experiment carbon was used because only one excited state is involved, thus making the calculations simpler. The angular distribution of neutrons escaping a 37 X 37 X 74 cm^3 block was measured by the time-of-flight technique. It was found not to be isotropic but to be peaked at angles around 50°. The experiment also was simulated on the IBM 7090 computer by the Monte Carlo method. Some changing of constants, which were determined by this method, will be required to get good agreement; but the basic fit is very encouraging, both for the angular distribution and for the "energy" distribution (in the form of a time-of-flight spectrum). Furthermore, the computer results show clearly that the unexpected angular distribution is due to the geometry of the carbon block. Calculations for a cubic block gave a forward peaked distribution.

ACKNOWLEDGMENTS

I should like to express my gratitude to my supervisor, Dr. J. M. Robson, for suggesting this interesting problem and for his able guidance throughout.

I should also like to thank Mr. B. Boraydn for writing some of the computer programs, and the McLennan Laboratory of the University of Toronto for use of the IBM 7090 computer.

CONTENTS

LIST OF FIGURES

List of Figures--Continued

1. INTRODUCTION

The initial idea for this investigation arose because of the lack of information on the usefulness or efficiency of concrete as a shield for installation such as the neutron generator at the University of Ottawa. This is the first part of an investigation into the mechanism by which fast neutrons are attenuated in large blocks of shielding materials. The general approach to this problem will be to measure experimentally the angular and the time-of-flight distributions of the neutrons which succeed in escaping from blocks of simple composition and shape which are placed in a beam of 14 Mev neutrons. The "energy" distribution computed from the time-of-flight distribution will be undetermined by $\pm\Delta E, \Delta E$ arising from the uncertainty of the neutrons' "history," which increases as the dimension of the block increases. A computation of the expected distributions will be made for these same blocks. If reasonable agreement can be achieved one will feel confident in using this type of calculation, which is much faster than the direct experimental approach, to extend the investigation to larger blocks of more

complicated composition.

Two basic methods may be used to do these calculations. The first one was developed mainly by R. E. Marshak[1] in conjunction with the application of the slowing down of fast neutrons to thermal energies to produce a chain reaction. The following assumptions are made: elastic scattering is isotropic in the center of mass system, and inelastic scattering is absent. A neutron distribution function $N(\vec{r},\vec{\Omega},u,t)$ is introduced, where $N(\vec{r},\vec{\Omega},u,t)d\vec{r},d\vec{\Omega},du$ is the number of neutrons between $\vec{r}$ and $\vec{r} + d\vec{r}$, $\vec{\Omega}$ and $\vec{\Omega} + d\vec{\Omega}$, u and u + du at time t, where $\vec{r}$ represents the radius vector, $\vec{\Omega}$ is a unit vector in the direction of the neutron velocity, and $u \equiv \ln(E_0/E)$, where E_0 is the initial energy (which is a constant since the source is monoenergetic) and E is the energy of interest. Then the time rate of change of $N(\vec{r},\vec{\Omega},u,t)$ is

$$\frac{\partial N}{\partial t}(\vec{r},\vec{\Omega},u,t) + \vec{v}\cdot\vec{\nabla}\, N(\vec{r},\vec{\Omega},u,t)$$

$$= - \frac{vN(\vec{r},\vec{\Omega},u,t)}{l(u)}$$

$$+ \int_0^u du' \; \frac{d\vec{\Omega}'v'N(\vec{r},\vec{\Omega}',u',t)xf(\vec{\Omega}'\cdot\vec{\Omega},\, u - u')}{l_s(u')}$$

where $\frac{1}{l(u)} = \frac{1}{l_s(u)} + \frac{1}{l_c(u)}$

and $l(u)$, $l_s(u)$, and $l_c(u)$ are the total, scattering, and capture mean free paths respectively. The first term on the right-hand side of the equation represents the number of scattering and capture collisions per unit time at $\vec{r}$ and t which are experienced by neutrons with parameters $\vec{\Omega}$ and u. The second term represents the neutrons scattered into the beam: $v'N(\vec{r},\vec{\Omega}',u',t)/l_s(u')$ is the number of neutron scatterings per second at $\vec{r}$ and t which are experienced by neutrons with parameters $\vec{\Omega}'$ and u'; $f(\vec{\Omega}'\cdot\vec{\Omega},u - u')$ is the relative probability of a neutron having parameters $\vec{\Omega}$ and u after a scattering collision, before which their values were $\vec{\Omega}'$ and u'.

The approximations are adequate for neutrons of about 2 Mev energy, which is the most probable energy of neutrons accompanying fission, but not for 14 Mev neutrons scattering from low A nuclei, where in general the elastic scattering is most probable in the forward direction and the first excited state lies between 4 and 6 Mev. Despite these approximations this method is by no means simple, as it involves solving an integral-differential equation. Furthermore, 2 Mev neutrons are well attenuated by few feet of concrete, while the most penetrating neutrons from fission are believed to be around 10 Mev; hence Marshak's method is not suitable to our problem. The second method is a Monte Carlo calculation.

and $l(u)$, $l_s(u)$, and $l_c(u)$ are the total, scattering, and capture mean free paths respectively. The first term on the right-hand side of the equation represents the number of scattering and capture collisions per unit time at $\vec{r}$ and t which are experienced by neutrons with parameters $\vec{\Omega}$ and u. The second term represents the neutrons scattered into the beam: $v'N(\vec{r},\vec{\Omega}',u',t)/l_s(u')$ is the number of neutron scatterings per second at $\vec{r}$ and t which are experienced by neutrons with parameters $\vec{\Omega}'$ and u'; $f(\vec{\Omega}'\cdot\vec{\Omega},u - u')$ is the relative probability of a neutron having parameters $\vec{\Omega}$ and u after a scattering collision, before which their values were $\vec{\Omega}'$ and u'.

The approximations are adequate for neutrons of about 2 Mev energy, which is the most probable energy of neutrons accompanying fission, but not for 14 Mev neutrons scattering from low A nuclei, where in general the elastic scattering is most probable in the forward direction and the first excited state lies between 4 and 6 Mev. Despite these approximations this method is by no means simple, as it involves solving an integral-differential equation. Furthermore, 2 Mev neutrons are well attenuated by few feet of concrete, while the most penetrating neutrons from fission are believed to be around 10 Mev; hence Marshak's method is not suitable to our problem. The second method is a Monte Carlo calculation.

The application of the Monte Carlo method to neutron scattering problems is mainly due to E. D. Cashwell and C. J. Everett.[2] This method consists in simulating what is happening to neutrons in a scattering material with a computer. To do this the computer must be provided with the following probabilities: (i) the probability that a neutron of energy E will travel a distance L before colliding; (ii) the probability that it will react with a particular type of nucleus if the scattering material is made up of more than one element; (iii) the probabilities for the various interactions that may occur, and (iv) the probability that a neutron will be scattered through an angle θ. With this information the computer using random numbers can calculate the distance travelled before the first collision occurs, the type of collision, the scattering angle and the energy of the scattered neutron, the distance from first to second collision, etc. When the neutron finally escapes from the scatterer, it is classified according to energy, time of flight, and laboratory angle at which it will be detected. The calculations are then repeated for other neutrons. If enough neutrons are processed the results are statistically reliable and can be compared with experiments. The time required for these calculations is not a limitation with high speed computers like the IBM 7090.

The Monte Carlo method was chosen to do the calculations because the mathematics used is very simple and the degree of approximations made can be changed at will without making the calculations any more difficult. Carbon was chosen as the first material to use in the experiments because the 4.4 Mev level is the only level with a high cross-section; the other levels are weak and thus do not complicate the calculations.

2. DESCRIPTION OF THE APPARATUS

The time-of-flight system used is of the associated particle type with one detector detecting the alphas (at 90° to the deuteron beam) produced by the $t(d,n)He^4$ reaction, the other one detecting the neutrons (see Fig. 1a). The pulses from the neutron detector in coincidence with the pulses from the alpha detector define a beam of neutrons (of mean energy of 14.2 Mev). The alpha detector consists of a plastic scintillator mounted on a CL 1090 photomultiplier. Fast pulses are obtained from the anode, which are then limited to prime and stop the timing apparatus and to feed one input of a fast coincidence circuit. Slow pulses are obtained from another dynode and are fed to a single channel analyzer (S.C.A.) through a cathode follower. The S.C.A. uses upper and lower discriminators to select those pulses which are due to alpha particles and not to protons from the $C^{12}(d,p)C^{13}$ and d(d,p)t reactions or to other background pulses.

The neutron detector consists of a 5"-diam. X 5"-long glass cell containing NE213 liquid scintillator mounted on a RCA 7046 photomultiplier. The photomultiplier was chosen for its high gain and high signal-to-noise ratio, the scintillator for its gamma discrimination property. Although gamma rays

are separated in time from 14 Mev neutrons by 16 nanoseconds per meter, if the scattering blocks are large enough some gamma rays will be counted on a time-of-flight spectrum as neutrons. Thus it was necessary to use a scintillator such as NE213 and to build a circuit that could discriminate between gammas and neutrons. The circuit diagram of the neutron pre-amplifier which the author built is shown in Fig. 1b. It consists of phase inverter with a 220-ohm load to match the 200-ohm line and two cathode followers of standard design with an output impedance of 100 ohms. From the second-last dynode, fast linear pulses are inverted and fed to a limiter which provides two output pulses, one 200 nanoseconds long to start the time to amplitude converter, the other one 10 nanoseconds long to be fed in coincidence with the fast alpha pulse. Slow pulses are taken from a lower dynode and fed to a S.C.A. through a cathode follower. The discriminators are set on these pulses to eliminate pulses due to cosmic rays and small pulses which do not trigger the time to amplitude converter for 200 nanoseconds. The pulses obtained from the last dynode which exceed a certain voltage level are indicative that they are due to neutrons; this is accomplished with Owen's method for pulse shape discrimination.[3]

The voltage between the last dynode and the anode is

maintained at a low value; consequently, during the high current portion of the pulse, space charge limits the current which can pass to the anode, and much of the multiplied charge cannot leave the last dynode, therefore driving it negative. During the decay part of the pulse, however, space charge limiting does not occur and a multiplied charge can pass to the anode. Whether the net charge on the dynode is positive or negative after each pulse depends on the relative amplitude of the fast and slow components. Since the decay component of a pulse due to proton recoil in NE213 is approximately twice as intense as for electron recoil, the voltage between the last dynode and anode is set such that the difference in pulse height between the most intense slow component of proton recoil pulses and the most intense slow component of electron recoil pulses is a maximum. This voltage for the RCA 7046 is found to be approximately 18 volts. These pulses are fed to a S.C.A. through a cathode follower. The fast component is limited and the pulses due to electron recoil are discriminated by raising the bias of the lower discriminator, the output of which triggers a flip-flop, thereby indicating that the event is due to a neutron. The effect of pulse shape discrimination can be seen in the time-of-flight spectra in Fig. 4.

The time-to-amplitude converter (see Fig. 2b), built by Mr. W. J. McDonald, is similar to that designed by J. S. Fraser and R. B. Tomlinson of A.E.C.L. The circuit consists of a capacitor, C_1, which is clamped to ground by two transistors, T_1 and T_2, that are normally on and another one, T_3, that is normally off, which act as an open circuit across the capacitor, C_1. When the alpha prime pulse arrives it turns T_1 off for at least 200 nanoseconds, but the capacitor does not charge until the neutron pulse turns T_2 off. The capacitor is then charged at constant current through a resistor, R_1, until the delayed (150 nanoseconds) alpha pulse turns T_3 on and discharges the capacitor through the resistance between the emitter and collector of the transistor. The constant current charging is accomplished by bootstrapping the resistor, R_1, so that the voltage on both sides of it falls at the same rate. The resulting pulse is not suitable to be analyzed by a multichannel analyzer because of the fast decay; hence, it is stretched by the 1N904 diode, R_2 and C_2, before being analyzed. The function of the prime pulse is to avoid having the capacitor charging when no alpha pulse is present. To eliminate events in which the start pulse precedes the prime pulse by less than 200 nanoseconds, coincidence is demanded between the prime and the 10 nanosecond-long pulse. The

discriminator output of all S.C.A. is fed into coincidence circuits, the outputs of which are used to gate the multichannel analyzer. Fig. 2a shows the block electronic diagram. The time-of-flight spectrum of the coincident neutron beam is shown in Fig. 3. The time resolution is seen to be 3.5 nanoseconds with the following contributions: detector and amplifier, 2.4 nanoseconds; electronics, 0.4 nanoseconds, and pulse amplitude, 2.5 nanoseconds. No pulse height compensation circuit was used; instead, the voltage on the focusing grid of the photomultiplier was adjusted (approximately 260 volts) to give the best time resolution. With the same detector and using a linear pulse height compensation circuit, the resolution would have been 3.3 nanoseconds.*

---

*W. J. McDonald, private communication.

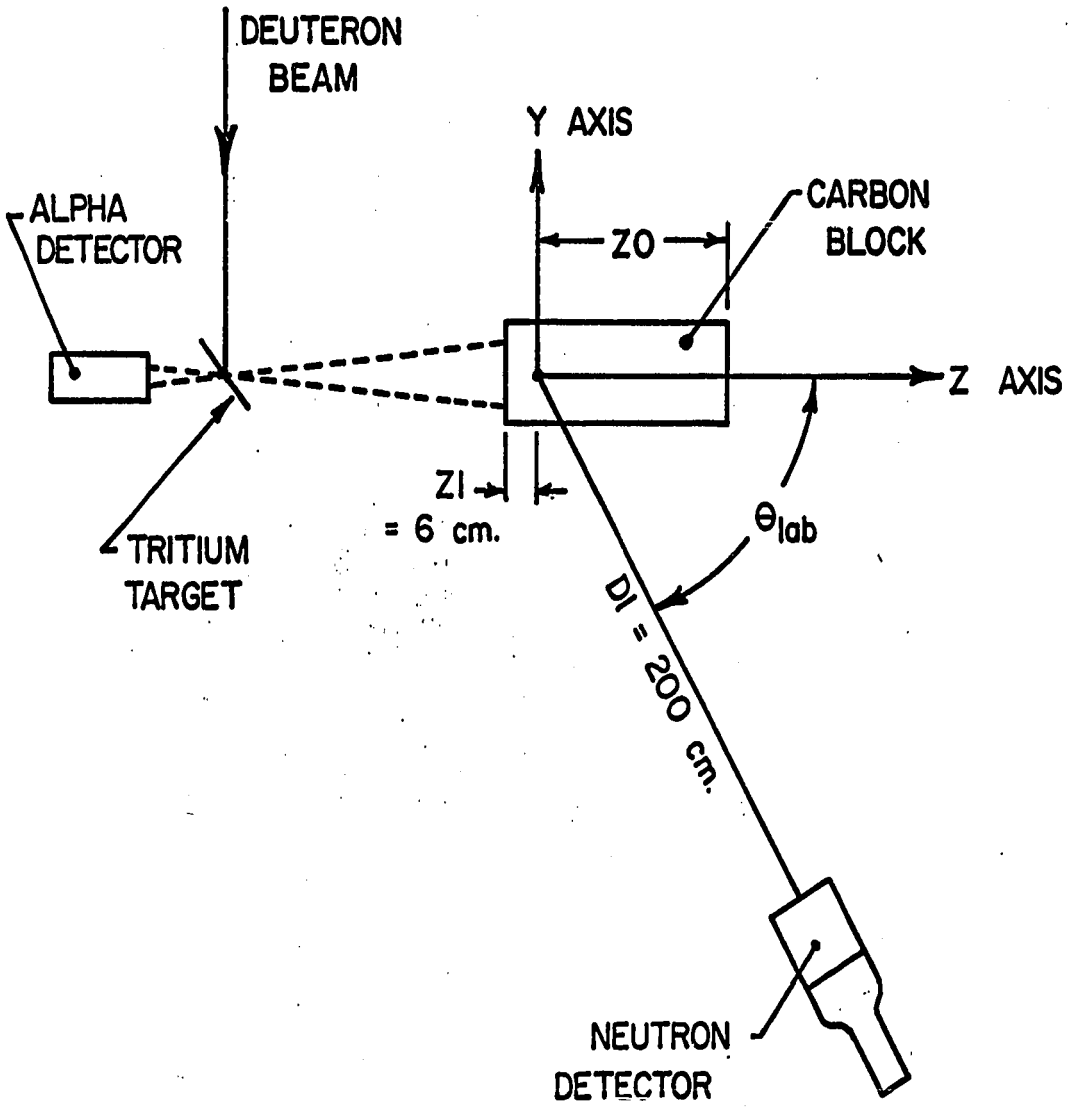

FIG. 1A GENERAL ARRANGEMENT OF APPARATUS

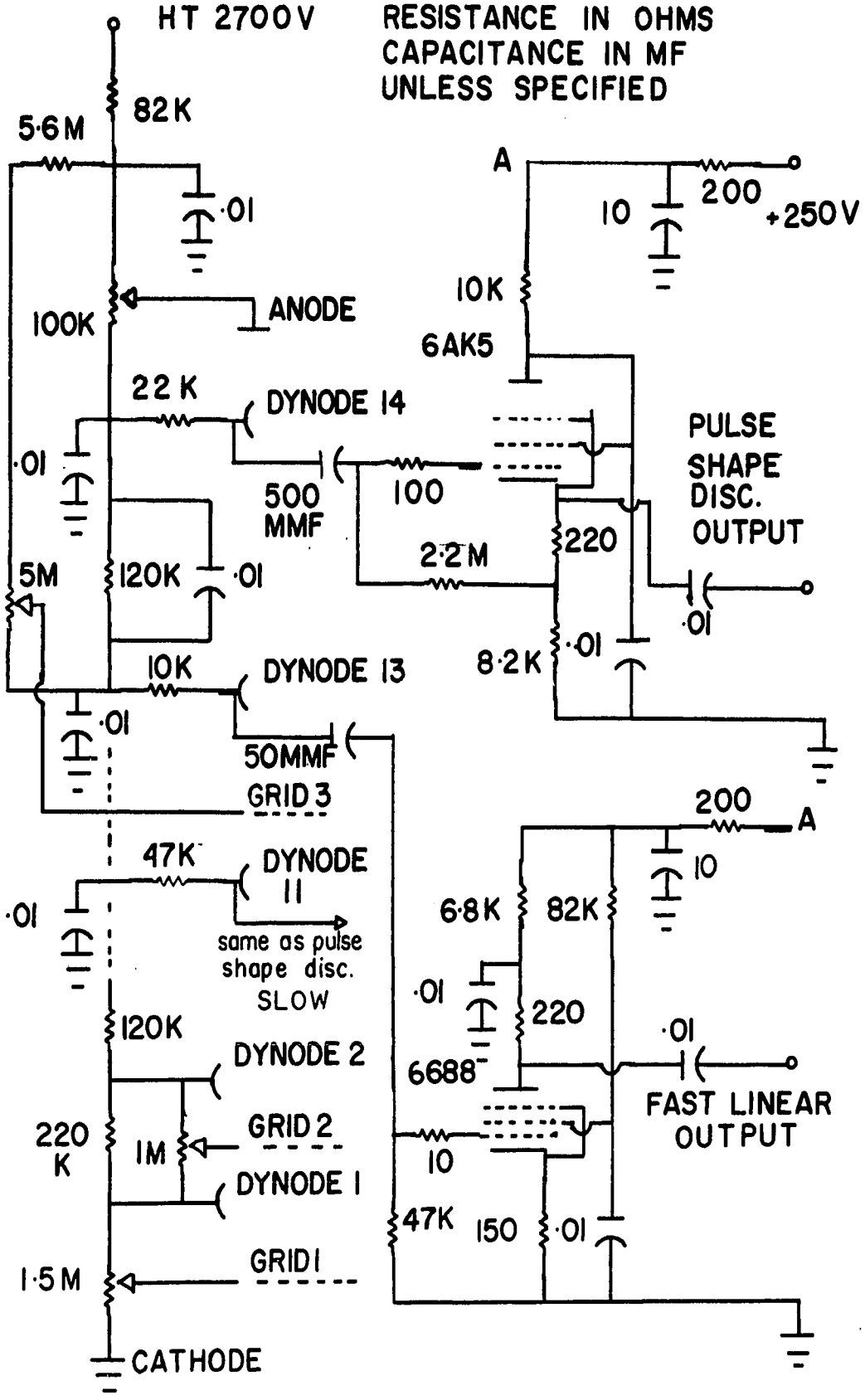

FIG 1B NEUTRON PREAMPLIFIER

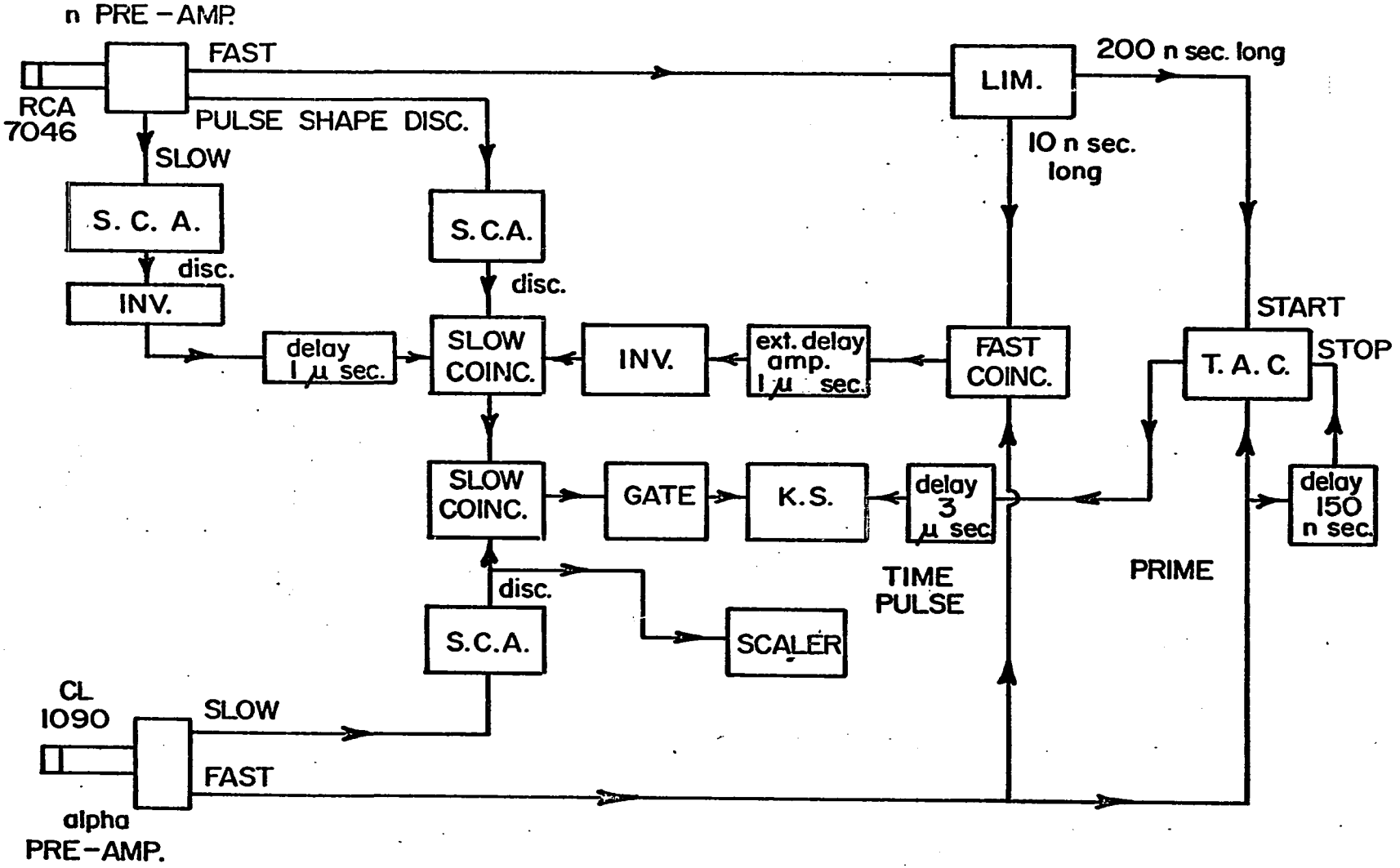

FIG. 2A BLOCK ELECTRONICS

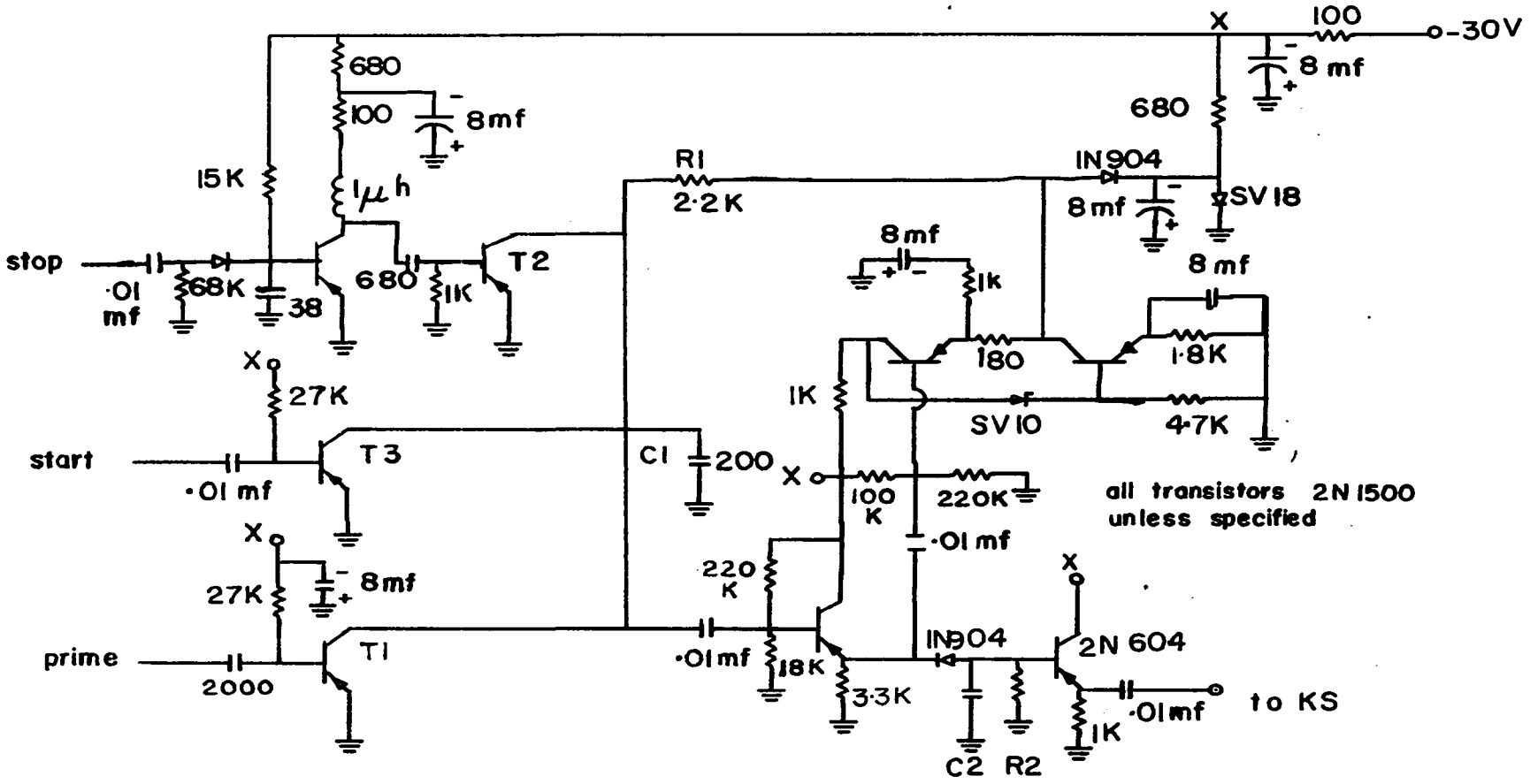

FIG 2B TIME TO AMPLITUDE CONVERTER

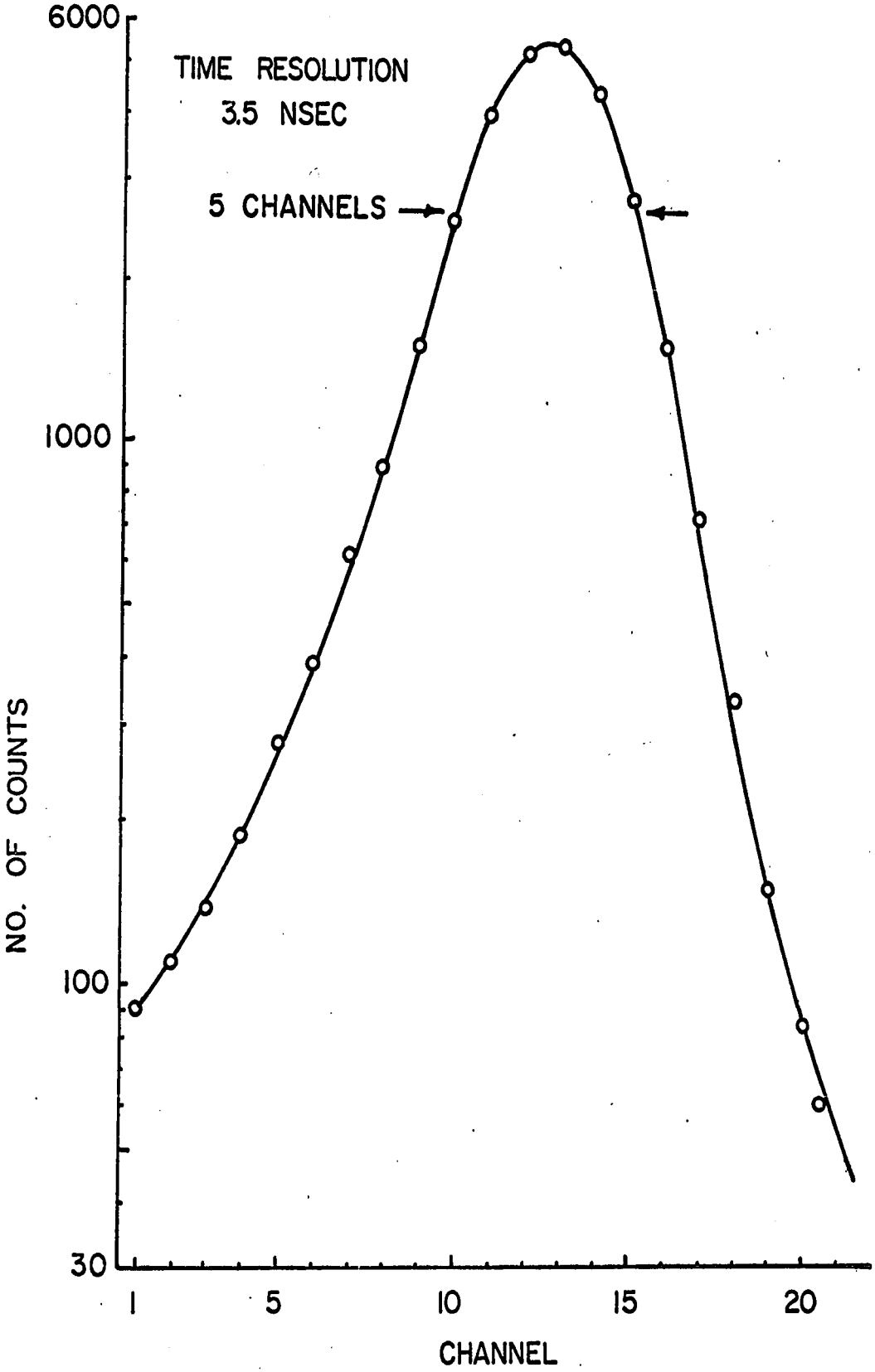

FIG. 3 TIME RESOLUTION OF THE APPARATUS

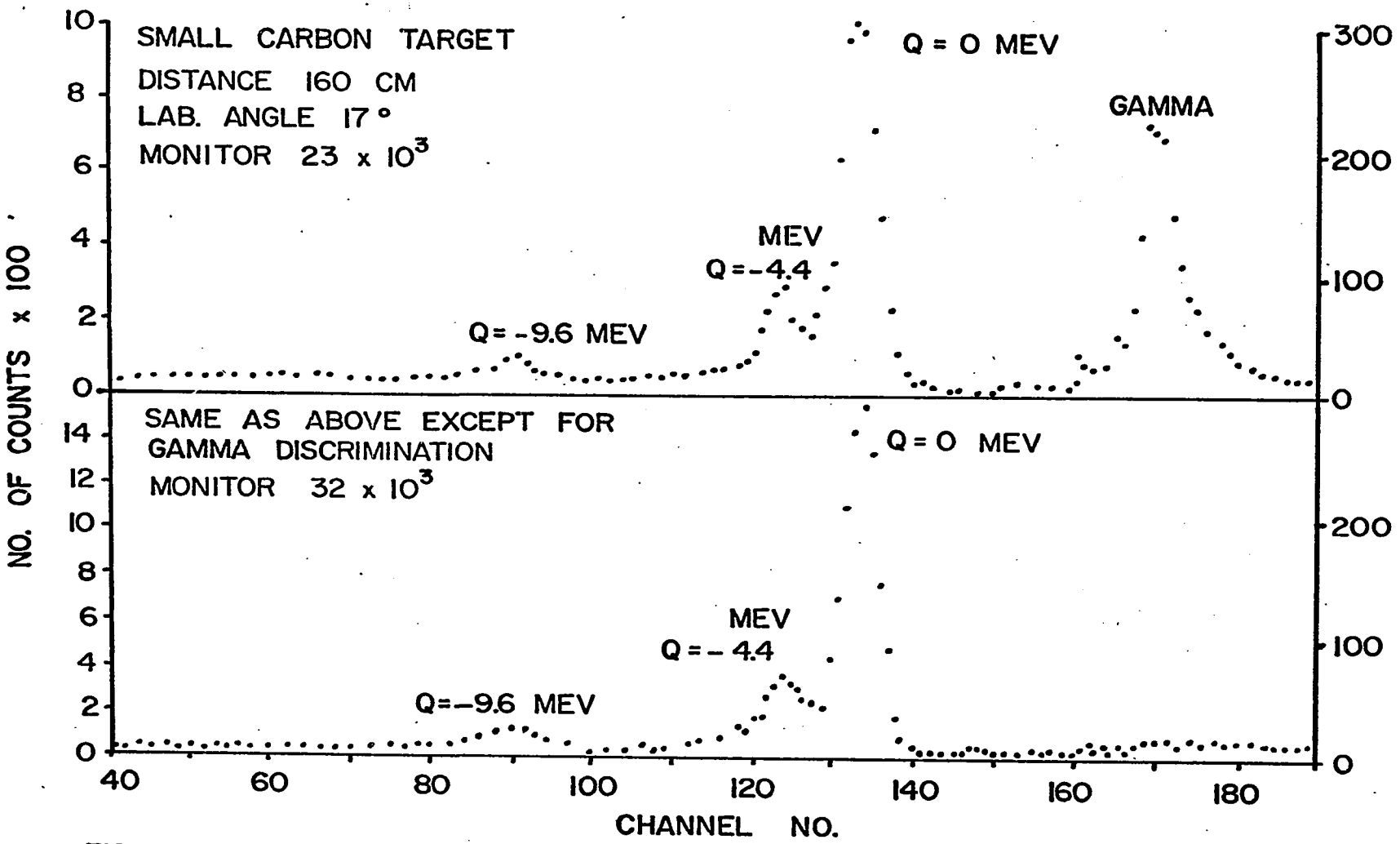

FIG. 4 EFFECT OF PULSE SHAPE DISC.

3. DESCRIPTION OF THE MONTE CARLO METHOD

Monte Carlo calculations are done using random numbers uniformly distributed on the interval $0 \leq r < 1$, which are used in the following manner to simulate stochastic processes.

Let us consider the case of a finite number of n independent events E(1),.....E(n) with probabilities P(1),..... P(n), such that $\sum_{i=1}^{n} P(i) = 1$; then if a number r lying in the interval (0,1) is chosen at random, such that

$$\sum_{i=1}^{s-1} P(i) \leq r < \sum_{i=1}^{s} P(i), \tag{1}$$

we will say the event E(s) has occurred. If N(s) is the number of times we have determined the event E(s) and N is the total number of random numbers chosen, then N(s)/N will approach P(s) as N approaches infinity.

Suppose that the number of events, n, approaches infinity such that the limit of

$$\sum_{i=1}^{s-1} P(i) - \sum_{i=1}^{s} P(i) \tag{2}$$

approaches zero as n approaches infinity for all values of s and $\sum_{i=1}^{n} P(i) = 1$, i.e. the probabilities are continuous.

Thus if x is a continuous variable in the interval (a,b), then

$P(1) = p(x_1)\Delta x_1$ = probability for x to lie between a and $a + \Delta x_1$

$P(2) = p(x_2)\Delta x_2$ = probability for x to lie between $a + \Delta x_1$ and $a + \Delta x_1 + \Delta x_2$

. . . . . .

. . . . . .

. . . . . .

$P(i) = p(x_i)\Delta x_i$ = probability for x to lie between $a + \Delta x_1 + \Delta x_2 + \Delta x_3 + \Delta x_{i-1}$, and $a + \Delta x_1 + \Delta x_2 + \Delta x_3 \ldots\ldots + \Delta x_i$, etc., and $\sum_{i=1}^{n} p(x_i)\Delta x_i = 1$. Then if we replace the P(i) in (1) by the above definitions and take the limit as n approaches infinity as defined in equation (2), we obtain

$$r = \int_a^x p(x)dx,$$

which determines x as a function of r. Since r is uniformly distributed on the interval (0,1), x is determined with frequency p(x)dx in the interval (x, x + dx).

To determine x as a function of r can lead to difficult implicit problems if the integral $\int_a^x p(x)dx$ is a complicated function of x. To overcome this difficulty, a technique devised by von Neumann is employed. It consists of throwing points (ξ, η) uniformly into the rectangle bounded by the lines x = a, x = b, y = 0, y = 1 and rejecting the points lying above the curve

$$y = p'(x) = p(x)/\max p(x),$$

x being assigned the value ξ whenever (ξ, η) falls below the curve. In many trials, the ratio of the number of points retained with ξ between x and x + dx to the number of points retained altogether will be approximately the ratio of the areas

$$p'(x)dx / \int_a^b p'(x)dx = p(x)dx / \int_a^b p(x)dx = p(x)dx.$$

For a more detailed description of the Monte Carlo method and its application to neutron scattering problems, see reference 2.

4. SIMULATION OF NEUTRON SCATTERING

In the laboratory a neutron beam with a rectangular cross section is incident on a carbon block which is placed at a distance R1 from the neutron source. The dimensions of the block are 2Xo in width, 2Yo in breadth, and Zo + Z1 in length. A coordinate system is chosen, with origin at a point inside the block at a distance Z1 perpendicular to the face of the block. Z1 is the distance at which the intensity of the incident beam drops to 50%. The X-Y plane is parallel to the face of the block. The neutron detector lies in the Y-Z plane at a distance DI from the origin (see Fig. 1a). The computer program can be divided into seven subprograms, which, for reference, will be named as follows: alpha, beta, gamma, delta, epsilon, iota, and omega.

In these seven subprograms the neutron history is calculated using the probability distribution of the possible events, as explained previously. In beta, the point where the neutron enters the block is calculated. In gamma, the point of first collision is determined. In delta, the type of process involved is determined, and if scattering occurs, the

scattering angle and the energy of the scattered neutron are calculated. In epsilon, the direction cosines of the scattered line of flight are calculated. In iota, the coordinates of the second or subsequent collisions are calculated and tested to determine whether the particle has escaped from the block. In omega, the laboratory angle at which the neutron will be detected is determined, and the neutron is classified according to energy, time of flight, and angle. In alpha, the neutrons are tallied in the proper counters.

Although a detailed description follows for a rectangular block composed of one element, the changes to be made for scatterers of different geometry and made up of many elements are obvious.

4a. Alpha

All the counters are set to zero if the experiment is a new one; if it is a continuation of a previous experiment, the last output is fed into the computer and the calculations are continued from the point where they left off. The total number of neutrons processed is also tallied; and when the desired number of calculations has been done, an output is printed.

4b. Beta

The direction cosines of the neutron as it leaves the source and the coordinates of the point where the neutron enters the block are calculated. The energy of the particle is an input constant. Since the neutron beam at a distance R1 from the source has a cross-sectional area 2P X 2Q, then the probability that the coordinate x of the neutron lies between x and x + dx is dx/2P. Thus

$$r = \int_{-p}^{x} dx/2P = (x + P)/2P$$

and

$$x = P(2r - 1).$$

Similarly,

$$y = Q(2r - 1)$$

and

$$z = -Z1.$$

The energy of the neutron is Eo and the direction cosines are:

$$U = x/R2$$

$$V = y/R2$$

$$W = R1/R2$$

where $(R2)^2 = (R1)^2 + x^2 + y^2$. The program then proceeds to "gamma."

4c. Gamma

The distance L travelled before a collision occurs is calculated using the mean free path for 14 Mev neutron in

carbon. Since the probability for a neutron to collide between L and L + dL is the product of the probability of a neutron travelling a distance L without colliding ($\exp -L/\lambda$, where λ is the mean free path) times the probability of colliding in dL (dL/λ), then

$$r = \int_0^L \frac{dL}{\lambda} \exp(-L/\lambda) = 1 - \exp(-L/\lambda)$$

and

$$L = -\lambda \ln(1 - r).$$

Since (1 - r) is uniformly distributed on $0 \leqslant r < 1$ if r is, then the equation can be simplified to

$$L = -\lambda \ln(r).$$

The coordinates of the point of collision can then be calculated and used to determine whether the collision occurred inside or outside the block. If the collision occurred outside, this neutron forms part of the transmitted beam and is tallied in counter NO; the program then returns to "alpha." If the neutron has collided inside, the time of flight for distance L is calculated, and the program proceeds to "delta."

Notice that the coordinates of the point of collision are calculated first and the type of collision later, instead of determining the type of collision first and then using the mean free path of the process involved to find the point of

collision. If we did this, the transmission obtained would be

$$\frac{\lambda(\text{total})}{\lambda_1}\exp(-x/\lambda_1) + \frac{\lambda(\text{total})}{\lambda_2}\exp(-x/\lambda_2) + \ldots\ldots$$

$\frac{\lambda(\text{total})}{\lambda_i}\exp(-x/\lambda_i)$, which is not equal to $\exp(-x/\lambda(\text{total}))$, the correct transmission.

4d. Delta

The neutron is classified according to its energy. The type of collision is determined by comparing a random number with the probabilities for elastic scattering, inelastic scattering, and reaction. If the event is a reaction, the neutron is tallied in counter NR, and the program proceeds to "alpha." If the event is a scattering, then by reference to the proper angular distribution the scattering angle $\cos^{-1}\mu$ is calculated using the von Neumann technique. The energy of the scattered neutron is calculated. If this energy is less than EB (bias energy), the neutron is tallied in counter NB, and the program proceeds to "alpha"; otherwise, the program proceeds to "epsilon."

4c. Epsilon

The angle $\cos^{-1}\mu$ calculated in "delta" defines a cone whose axis is in the same line as the incident line of flight. Since the neutrons are not polarized, i.e. their spin has no

preferred direction, they are uniformly distributed on this cone. If we were looking at a certain time, t, along the axis of this cone, we would see neutrons uniformly distributed on a circle. Let us draw any radius as reference and call the angle δ the angle between the radius vector $\vec{r}$, which defines the position of a neutron on the circle, and our reference radius. Then the probability that the angle δ lies between δ and $\delta + d\delta$ is $d\delta/2\pi$; hence

$$r = \int_{-\pi}^{\delta} d\delta/2\pi = \frac{\delta + \pi}{2\pi}$$

and

$$\delta = \pi(2r - 1).$$

Which radius we take as reference does not matter because the neutrons are uniformly distributed in δ. The direction cosines of the scattered line of flight with respect to the coordinate system are calculated using transformation formulas; for details see reference 2. The program then proceeds to "iota."

4f. Iota

To calculate the distance travelled from first to second collision, the neutron is classified according to the energy so that the appropriate mean free path is used. The

coordinates of the point of second collision are then calculated and compared with the dimensions of the block. If the collision occurred outside the block, the program proceeds to "omega." If the collision occurred inside, the time taken to travel between collisions is calculated, and the program returns to "delta." This repeats until the neutron either escapes from the block or is tallied in a counter.

4g. Omega

The direction cosine W' calculated in "epsilon" is the cosine of the angle between the line of flight of the escaping particle and the z-axis of the system. Since in the laboratory the angles are measured with respect to the origin, and the distance from the origin to the detector is finite, the angle defined by W' does not correspond to the angle at which this neutron is detected in the laboratory unless the line of flight of the escaping neutron and the origin lie in a straight line. Therefore, it is necessary to take into account that a neutron escaping from the block with direction cosine W' and the coordinates of the point of last collision being (x', y', z') will be detected by a detector band at a distance DI from the origin at an angle $\cos^{-1}W$. The relation between W' and W is the following:

Let S be the projection of the vector $x'\vec{i} + y'\vec{j} + z'\vec{k}$ on the unit vector (U',V',W'), then

$$S = U'x' + W'z' + V'y'.$$

Let t be the distance of the line of flight from (x',y',z') to the detector band, and let S' = t + S, then

$$(S')^2 = (DI)^2 - (x')^2 + (y')^2 + (z')^2 - S^2$$

and

$$t = S' - S$$

the z coordinate of the point where the neutron is detected $z_f = z' + W't$, and $W_f = z_f/DI$.

The neutron is then classified according to angle, energy, time of flight, and tallied in the proper counters. The program then returns to "alpha," and the calculations are repeated for another neutron.

5. DESCRIPTION OF PROBLEMS RUN ON COMPUTER

The logic or flow chart for the calculations was written by the author. Mr. Boraydn translated the flow chart for the IBM 650, where an amount of testing and simulation have been done. This computer was too slow and so it was decided to use the IBM 7090, which for our calculations was found to be six hundred times faster than the IBM 650. The 7090 program was written by the IBM company; later, modifications were made by the author.

The random number generator used has a periodicity of 2^{28}; the best starting value is 0.5. This subroutine has been tested and used many times at the McLennan Laboratory with different problems, and so far it has given satisfactory results.

To test the program we simulated scattering from a thin carbon sample. Ten thousand neutrons were started according to beam B of Fig. 10. A comparison between the elastic angular distribution fed into the computer and the calculated one is shown in Fig. 9. The statistical error is 10% at medium angles; elsewhere it is greater than 10%.

The attenuation of the incident flux through the scattering sample is given by $(1 - \exp(-t/\lambda))\ \lambda/t$. It is very simple to calculate it for a slab with the neutrons incident in a parallel beam, but if the neutron source is a point source and the scatterer is cylindrical in shape it is not so easy to calculate the attenuation without making approximations. The transmission through the polyethylene sample was calculated. This gives a value of $\exp(-t/\lambda)$, determining an effective t and the attenuation factor.

The efficiency of the neutron detector is defined as the number of neutrons detected divided by the number of neutrons incident on the detector. It is measured in the laboratory by measuring the angular distribution of neutrons scattered by hydrogen. Since this angular distribution is well known, the efficiency of the neutron detector for various energies is obtained in a straightforward manner. This efficiency is underestimated because of multiple scattering. Due to unforeseen circumstances, this experiment was not simulated with the computer; instead, some simple estimates were done. The polyethylene sample used was cylindrical in shape. If chords of a circle of radius R are drawn perpendicular to one diameter, it is found that the average length of this chord is $\pi R/2$. The following assumption was made: after one collision, the

neutrons had to traverse a distance $\pi R/4$ through the polyethylene before escaping. Hence, $\exp\left[-n_H\sigma_H(E) - n_C\sigma_C(E)\right]\frac{\pi R}{4}$ gives the fraction of scattered neutrons of energy E which were not multiply scattered, where n and $\sigma(E)$ are the density of nuclei and the total cross-section for neutrons of energy E. The subscripts H and C refer to hydrogen and carbon nuclei, respectively. The second assumption is that the multiply scattered neutrons can be ignored. With these assumptions our efficiency results must be multiplied by $\exp\left[n_H\sigma_H(E) + n_C\sigma_C(E)\right]\frac{\pi R}{4}$. The effect of the second assumption is to overestimate the efficiency by $\delta/\exp\left[-n_H\sigma_H(E) - n_C\sigma_C(E)\right]\frac{\pi R}{4}$ X 100%, where δ is the contribution from multiply scattered neutrons; δ can be calculated by a Monte Carlo calculation. δ is small compared to the denominator for high-energy neutrons. At lower energies, it may become significant; but because of the energy uncertainty due to the geometry of the experiment, nothing is gained by correcting the efficiency in a much more laborious manner, unless it can be done quickly with a computer.

The differential cross-sections used for the calculations with the large carbon blocks are shown in Appendix A. To save storage space the angular distributions were fed into the computer as polynomials. They were obtained by fitting the

angular distributions by the least-square method. The computer calculated the coefficients of the polynomials (see Appendix B), but it was necessary to specify the powers of the independent variable involved. The total cross-sections and the cross-sections for elastic, inelastic, and reaction were averaged over the energy intervals, i.e.

$$\overline{\sigma}_i = \int_{E_{i+1}}^{E_i} \sigma(E)dE / E_i - E_{i+1}$$

With these data, calculations were made for a 37 X 37 X 37 cm^3 and a 37 X 37 X 74 cm^3 carbon block. For both these calculations, 150,000 neutrons were processed in one hour.

6. DESCRIPTION OF EXPERIMENTS

(a) Neutron Detector

An aluminum container was built to hold the liquid scintillator. To seal it, a neoprene O-ring or, alternatively, a teflon gasket was used, both unsatisfactorily. The former released impurities; the latter did not make a tight seal. Consequently, a liquid scintillator already encapsulated in a glass cell was bought from Nuclear Enterprises (Canada) Ltd.

(b) Pulse Shape Discriminator

As it was important to have sufficient gain in the photomultiplier that low energy neutrons would trigger the time-to-amplitude converter, it was desirable to try a method of pulse shape discrimination which does not use the anode of the photomultiplier. The method of J. Reithmeier *et al.*[10] accomplishes this; furthermore, it uses pulses from one dynode only, while other methods use pulses from two dynodes. Pulses are taken from a dynode and inverted; they then appear across a load which matches one end of a clipping cable, the other end of which is terminated by a resistance somewhat smaller

than the intrinsic impedance of the cable, so that there will be a reflection. Since the intensity of the slow component of pulses due to gamma rays is half that of pulses due to neutrons, the length of cable and terminating resistor can be chosen such that for gamma rays there will be a positive swing. This can then be used to trigger an anticoincidence circuit to detect the neutrons. This method was tried but not found to be successful. It was then decided to use Owen's method and to obtain a fast pulse for the time-to-amplitude converter from the second-last dynode. This was found to be satisfactory.

The bias in the pulse shape discrimination system was adjusted so that 95% of the gamma rays, of 2.6 Mev energy from a ThC source, was rejected. The bias in the neutron S.C.A. was adjusted so that the 0.66 Mev gamma rays from Cs^{137}, which give pulse heights equivalent to 2 Mev neutrons, could just be detected.

The experimental set-up was checked by measuring the elastic differential cross-section of neutrons scattered by a carbon sample 2 cm thick having a cross-section area of 18 X 18 cm^2 with a 2" X 2" NE213 scintillator and a 6342 photomultiplier. The sample was placed in the neutron beam according to the beam measurements taken by W. J. McDonald. Measurements were taken

than the intrinsic impedance of the cable, so that there will be a reflection. Since the intensity of the slow component of pulses due to gamma rays is half that of pulses due to neutrons, the length of cable and terminating resistor can be chosen such that for gamma rays there will be a positive swing. This can then be used to trigger an anticoincidence circuit to detect the neutrons. This method was tried but not found to be successful. It was then decided to use Owen's method and to obtain a fast pulse for the time-to-amplitude converter from the second-last dynode. This was found to be satisfactory.

The bias in the pulse shape discrimination system was adjusted so that 95% of the gamma rays, of 2.6 Mev energy from a ThC source, was rejected. The bias in the neutron S.C.A. was adjusted so that the 0.66 Mev gamma rays from Cs^{137}, which give pulse heights equivalent to 2 Mev neutrons, could just be detected.

The experimental set-up was checked by measuring the elastic differential cross-section of neutrons scattered by a carbon sample 2 cm thick having a cross-section area of 18 X 18 cm^2 with a 2" X 2" NE213 scintillator and a 6342 photomultiplier. The sample was placed in the neutron beam according to the beam measurements taken by W. J. McDonald. Measurements were taken

from 15° to 90° inclusive, in steps of 15°. The experimental results were corrected for attenuation of the incident neutron flux through the sample and absorption of neutrons scattered at large angles, but not for multiple scattering, as its effect should be small due to the thickness of the sample. The results obtained are compared with those obtained by Anderson et al.[4] in Fig. 7.

The differential cross-section for n-p scattering was measured using a polyethelyne sample 5 cm in diameter X 10 cm in length. As the differential cross-section is known and the scattering angle Θ_{lab} is related to the energy E of the scattered neutron by $\Theta_{lab} = \cos^{-1}(E/E_o)^{1/2}$, where E_o is the energy of the incident neutron, then the ratio between the measurement at each scattering angle and the expected value gives the efficiency as a function of energy.

A typical time-of-flight spectrum is shown in Fig. 5. The width of the peak, corresponding to neutrons scattered from hydrogen, is due to the width of the incident neutron beam. When necessary, a subtraction was made for the scattering from carbon. The differential cross-section obtained was corrected for multiple scattering and attenuation of the incident flux through the scatterer. The efficiency of the detector as a function of energy is shown in Fig. 6.

The neutrons escaping from a 37 X 37 X 74 cm^3 carbon block were detected at a distance of 2 meters from the origin of the coordinate system described in section 4. Typical time-of-flight spectra are shown in Figs. 11, 12, and 13. To obtain an absolute value of the angular distribution shown in Fig. 14, an efficiency of 33% was used for all neutrons irrespective of their energy. This value was obtained by averaging the efficiency according to the energy distribution calculated by the computer.

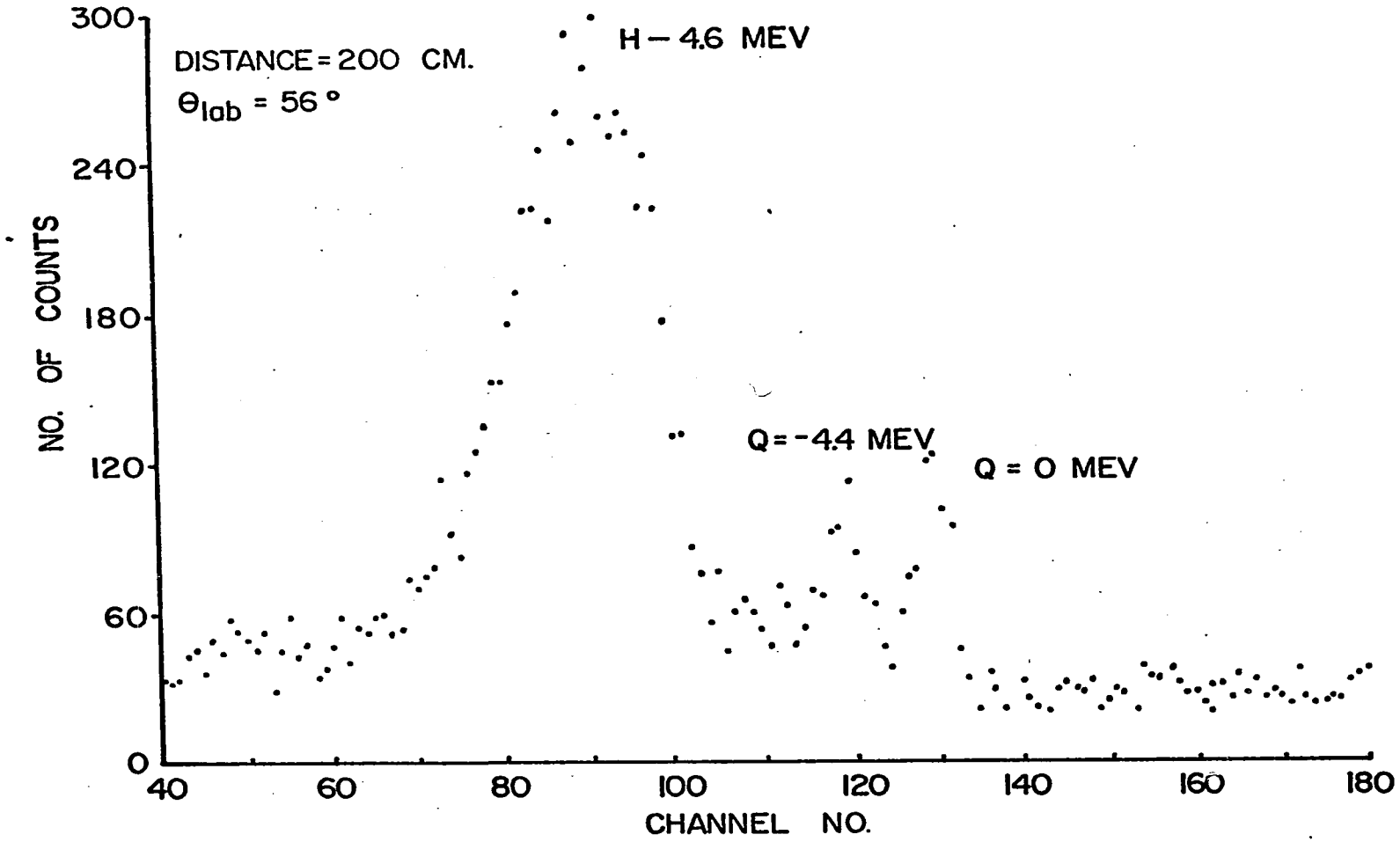

FIG. 5 SCATTERING FROM CH_2

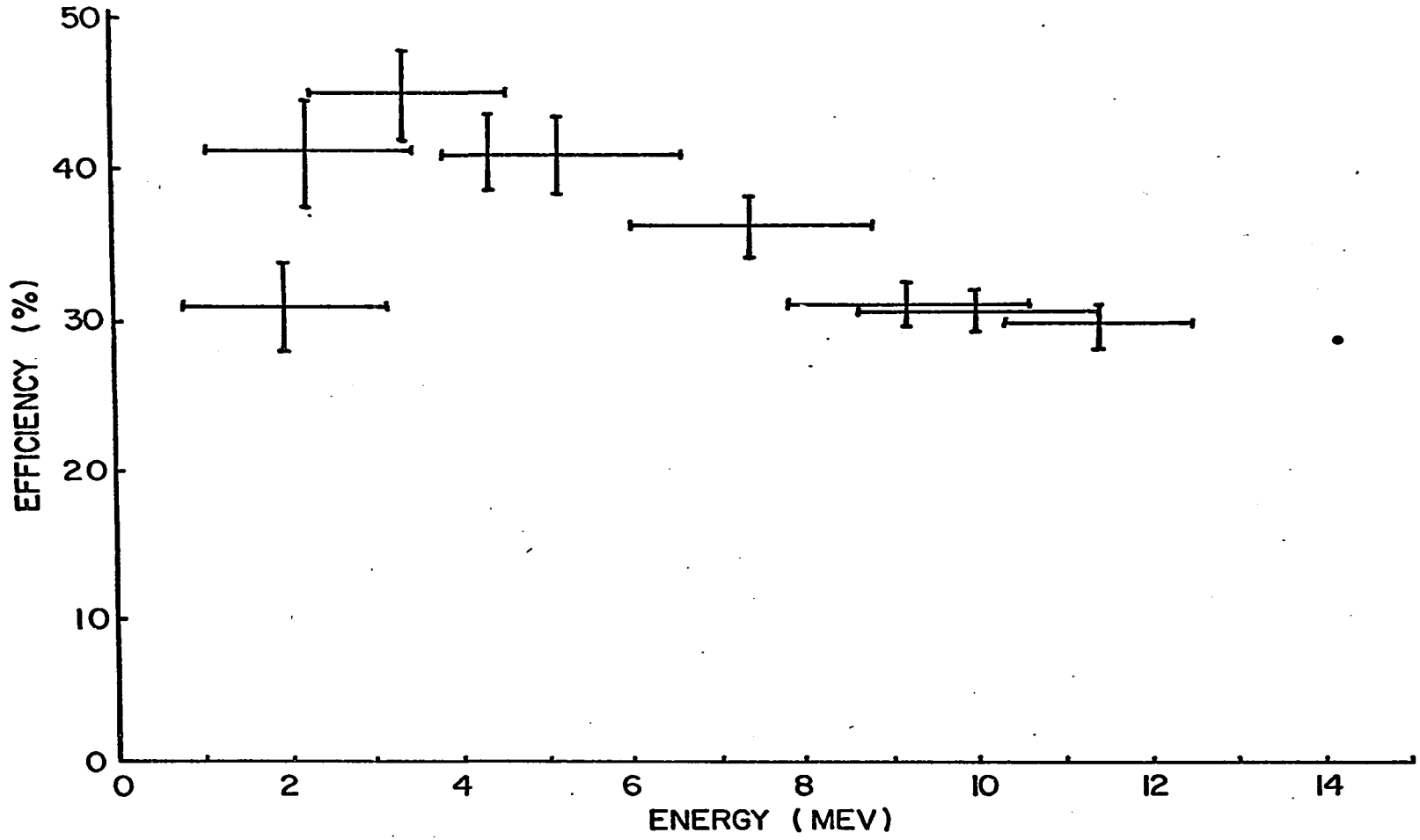

FIG. 6 EFFICIENCY CALIBRATION OF NEUTRON DETECTOR

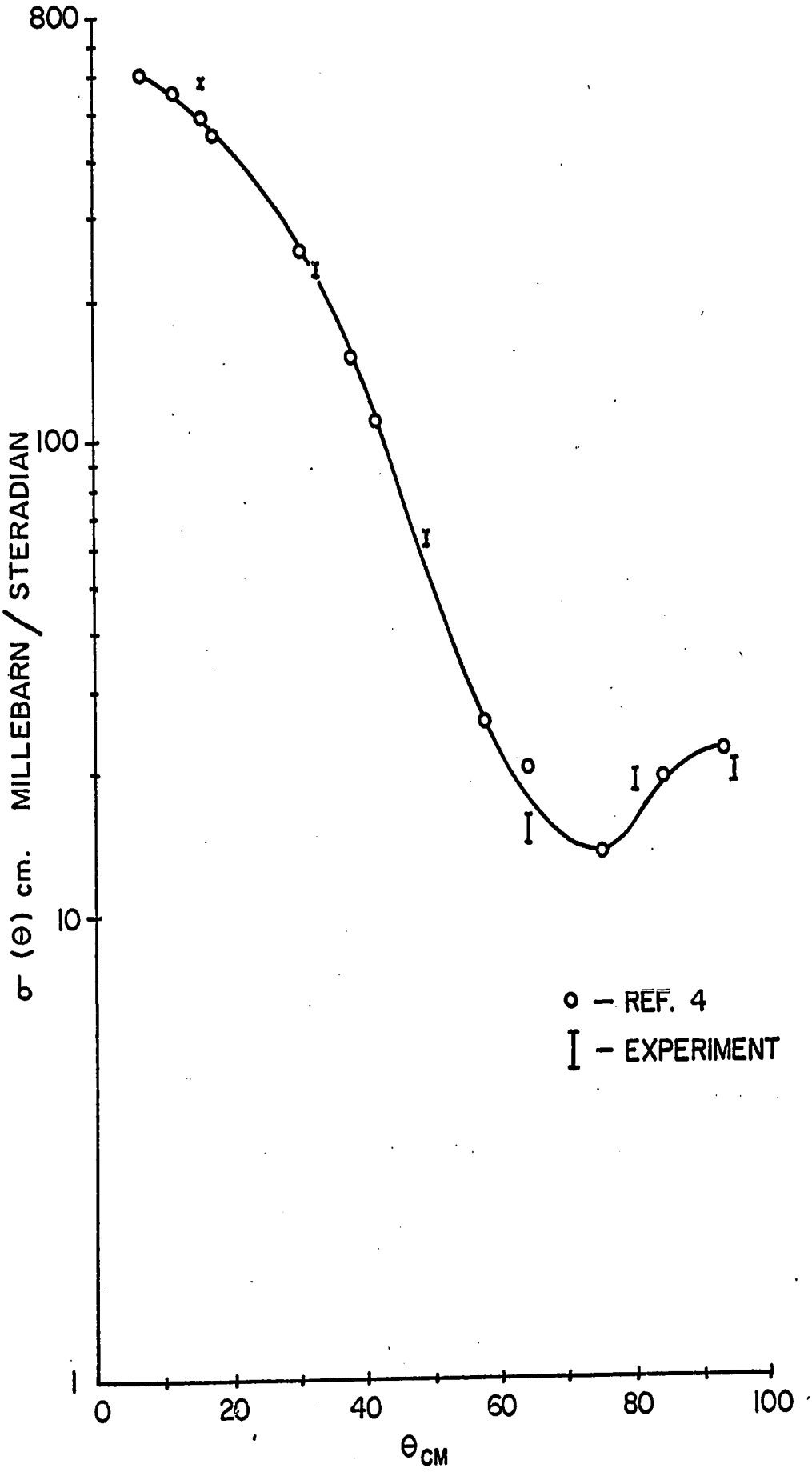

FIG. 7 ELASTIC DIFFERENTIAL CROSS SECTION MEASURED WITH A THIN CARBON SCATTERER.

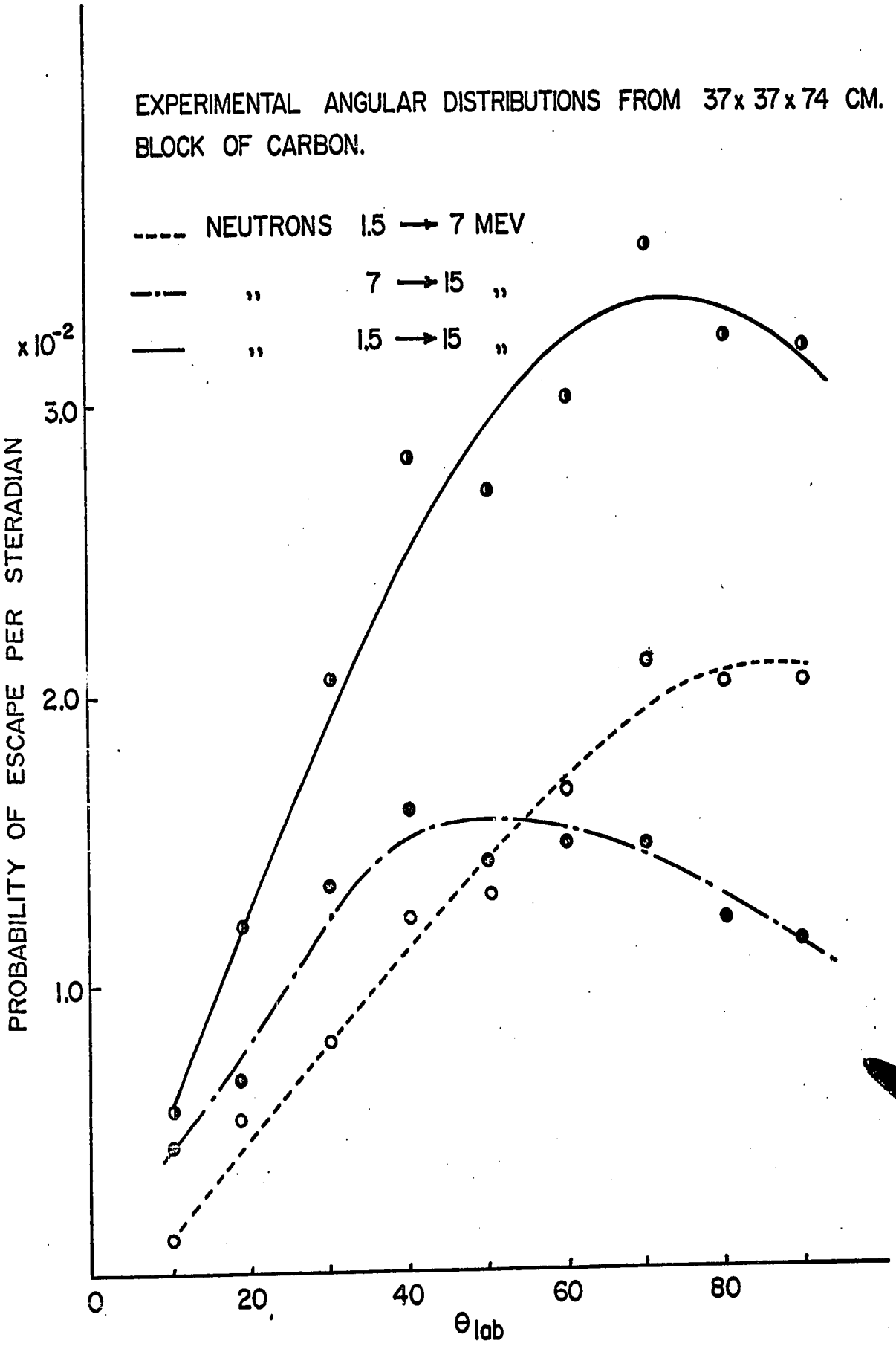

FIG. 8 SCATTERING FROM THE THICK BLOCK OF CARBON

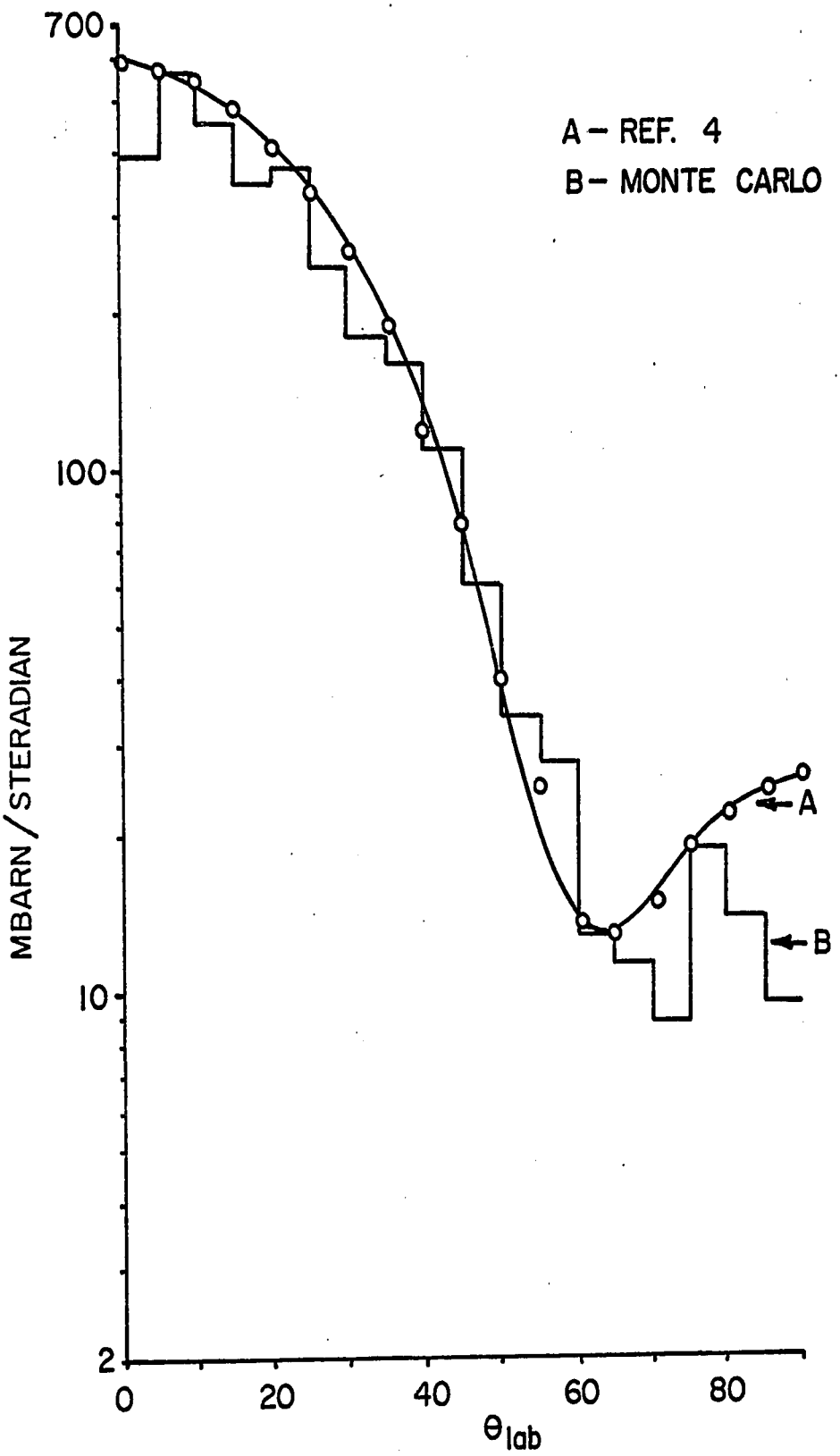

FIG. 9 ELASTIC DIFFERENTIAL X – SECTION COMPARISON WITH EXPERIMENT (4) OF MONTE CARLO RESULTS FOR A THIN BLOCK.

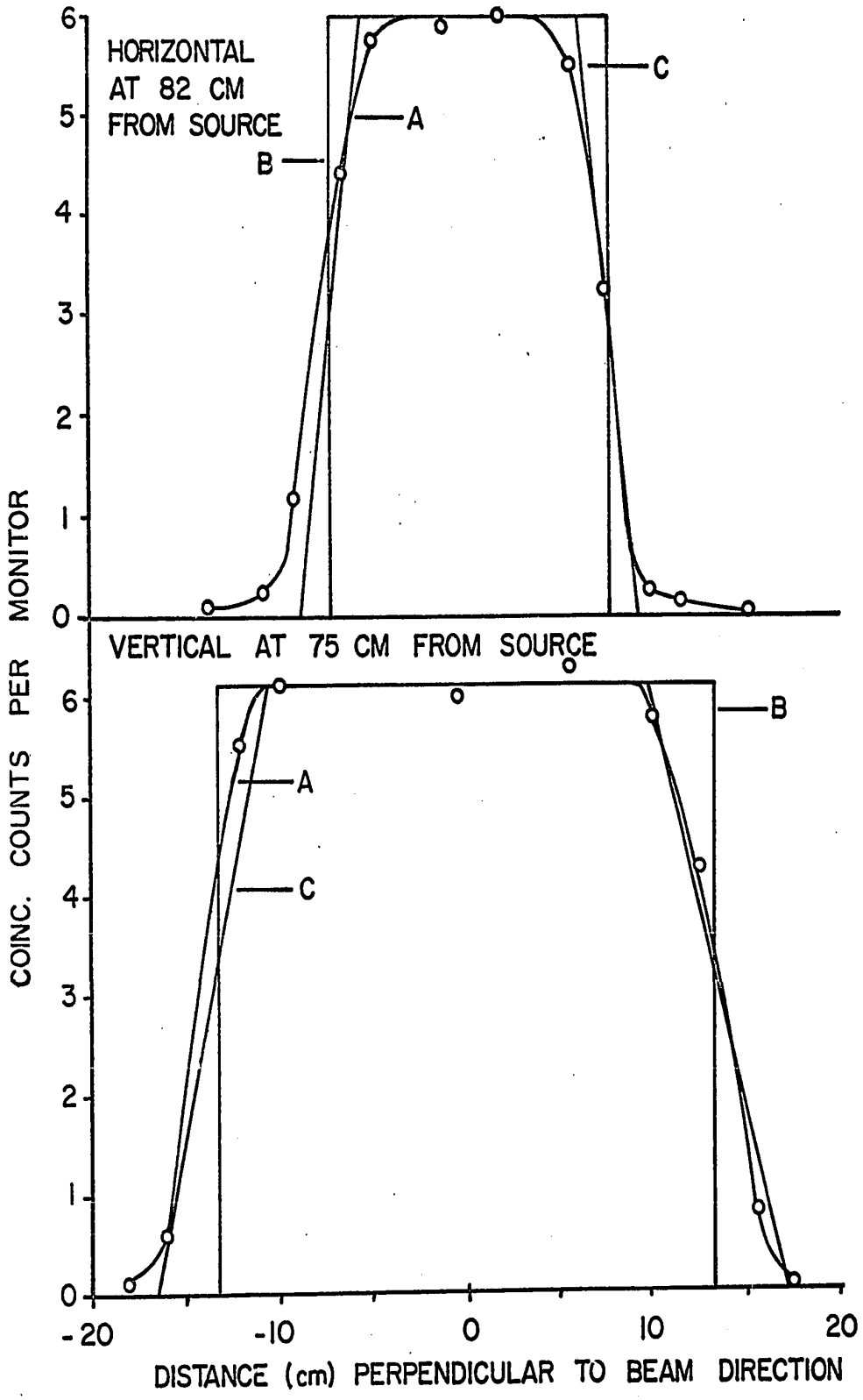

FIG. 10 BEAM PROFILE

7. DISCUSSION

Fig. 14 shows the experimental and calculated angular distribution of neutrons escaping a carbon block 37 X 37 X 74 cm^3, with the neutron beam incident on the 37 X 37 cm^2 side. The curves do not fit very well, especially at large angles. These calculations were made with the neutron beam B of Fig. 10. Fig. 15 shows the results when beam C is used; the curves fit better for $\theta_{lab} \leq 50°$, but there is no improvement at larger angles. A qualitative description of the shape of the angular distribution can be made in terms of multiple scattering (not multiple collisions), absorption, and geometry of the sample. Although the differential scattering (elastic and inelastic) cross-section for single scattering of neutrons is very predominant in the forward direction, multiple scattering decreases the flux moving in the forward direction while increasing the flux moving laterally until the flux is isotropic. The carbon block used in our experiment is approximately 9 m.f.p. (mean free path) long for 10-14 Mev neutrons. Suppose that we had used a block 9 m.f.p. long with a cross-sectional area of 18 m.f.p. X 18 m.f.p., then the angular

distribution would be isotropic or nearly so. The distance from the spot where the incident beam hits the block to the periphery is approximately constant, so that the probability for absorption is the same for all neutrons. If we decrease the cross-sectional area of the block but keep the length constant, the absorption will no longer be the same for all neutrons but will depend on the direction in which the neutrons are moving. Let a_L, a_M, a_S be the probability for absorption of neutrons moving towards large, medium, small angles respectively, and let S_L, S_M, S_S be the probability for scattering neutrons out of the neutron flux moving towards large, medium, and small angles respectively, then due to the geometry of the sample

$$a_L < a_M < a_S$$

and

$$S_L < S_M < S_S$$

Thus the angular distribution for a carbon block 9 m.f.p. long with a cross-sectional area of 9 m.f.p. X 9 m.f.p. should be a maximum at large angles and decreasing as the angle decreases. This is roughly what is observed. Fig. 18 shows the calculated angular distribution for a 37 X 37 X 74 cm^3 and 37 X 37 X 37 cm^3 sample with a 1 Mev bias; the effect of absorption in the

forward direction is clearly seen. In Figs. 16 and 17, the energy spectrum at four angles is shown. At forward angles the neutron density from 8 Mev to 14 Mev is greater than from 1 Mev to 8 Mev. As the angle increases the density at higher energy decreases while at lower energy it increases. This is more clearly seen in Fig. 8. The time-of-flight spectra are compared in Figs. 11, 12, and 13. The fit is better for the last 50 channels than for the first 70, where the experimental spectra are higher than the calculations. The time-of-flight spectra were calculated for four nanosecond intervals. To compare them with spectra seen with the multichannel analyzer it was assumed that the time calibration was constant and equal to 0.7 nanoseconds per channel. This is not exactly true below channel 70 but introduces a negligible error.

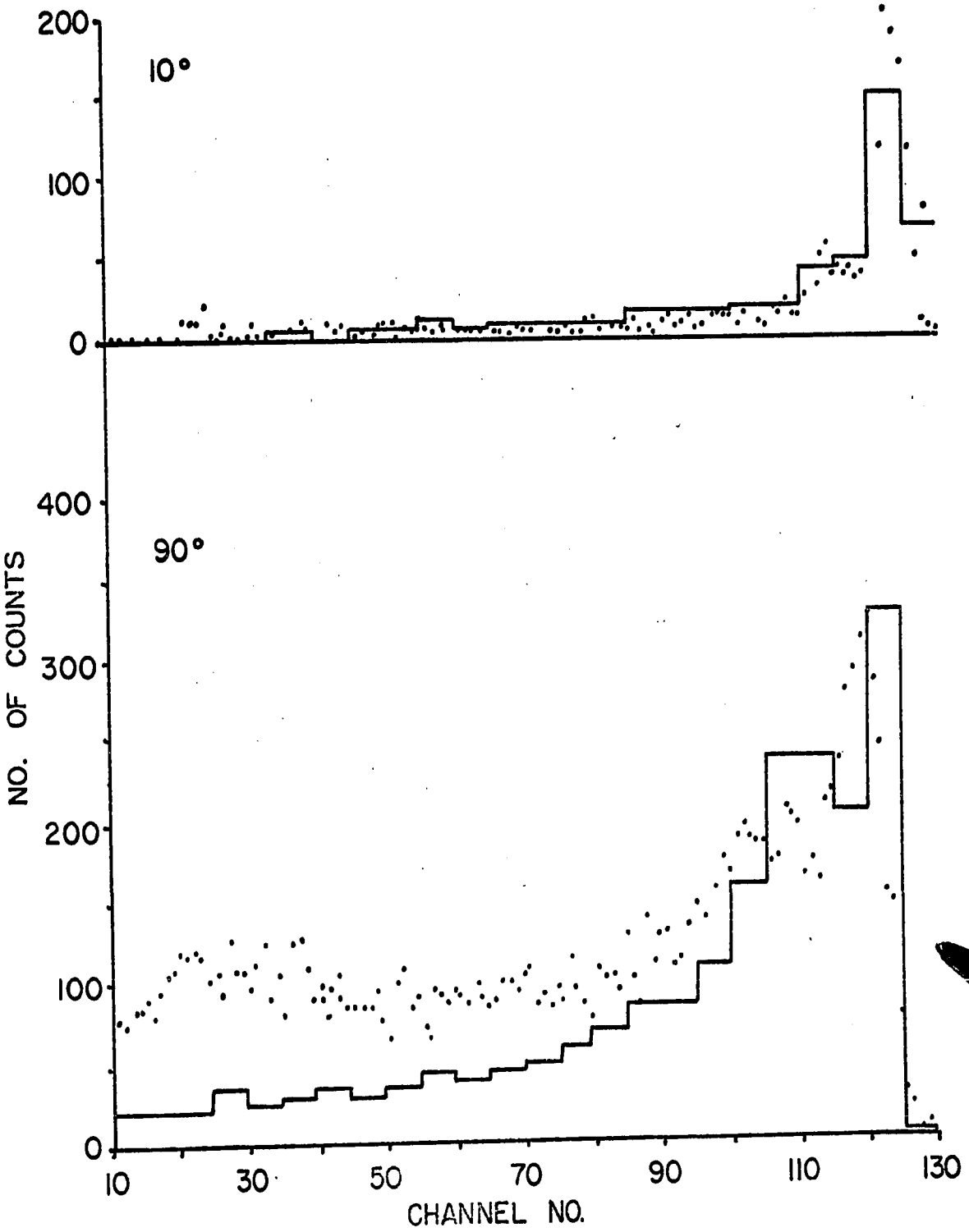

FIG. 11 COMPARISON OF TIME OF FLIGHT SPECTRA

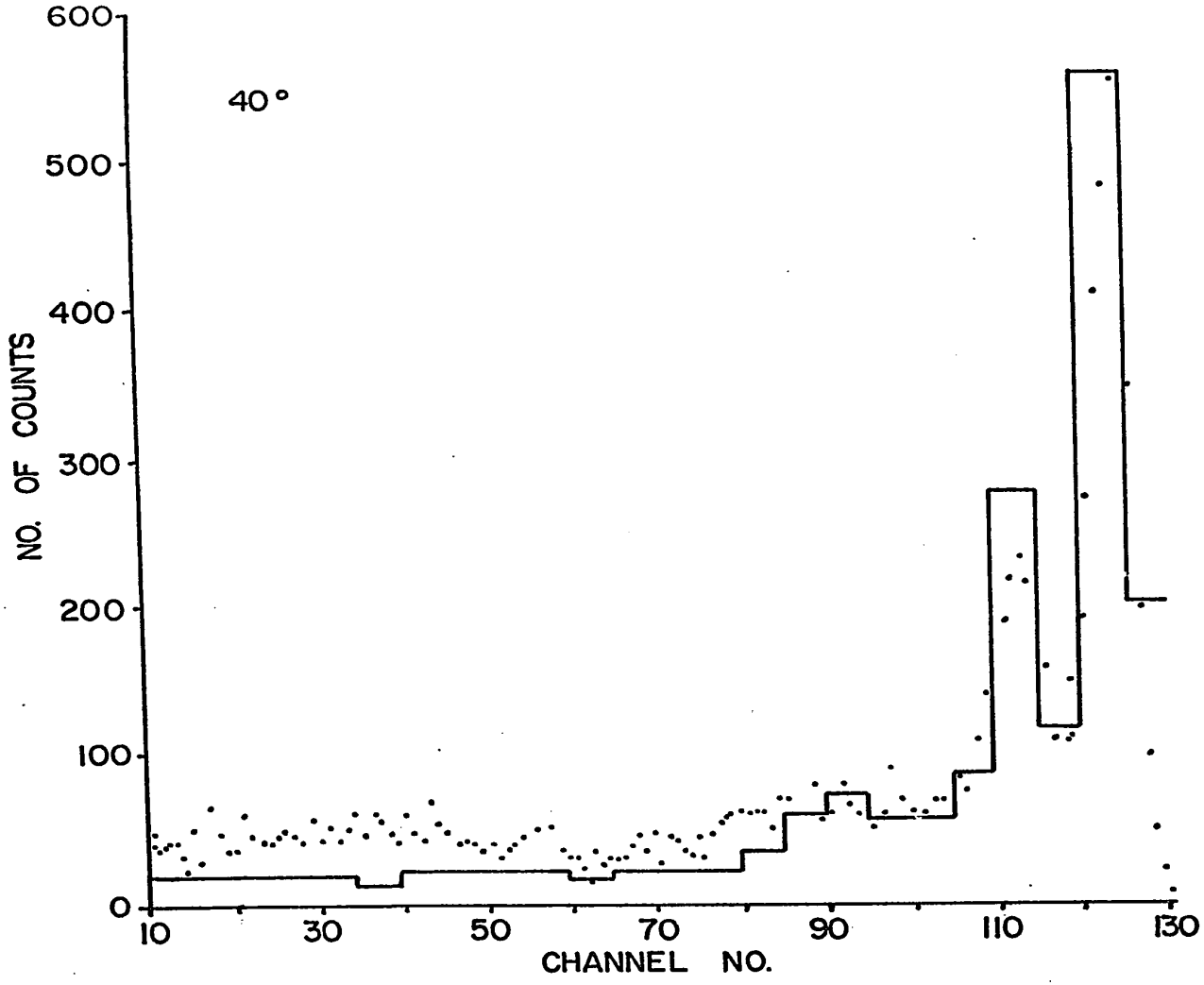

FIG. 12 COMPARISON OF TIME OF FLIGHT SPECTRA

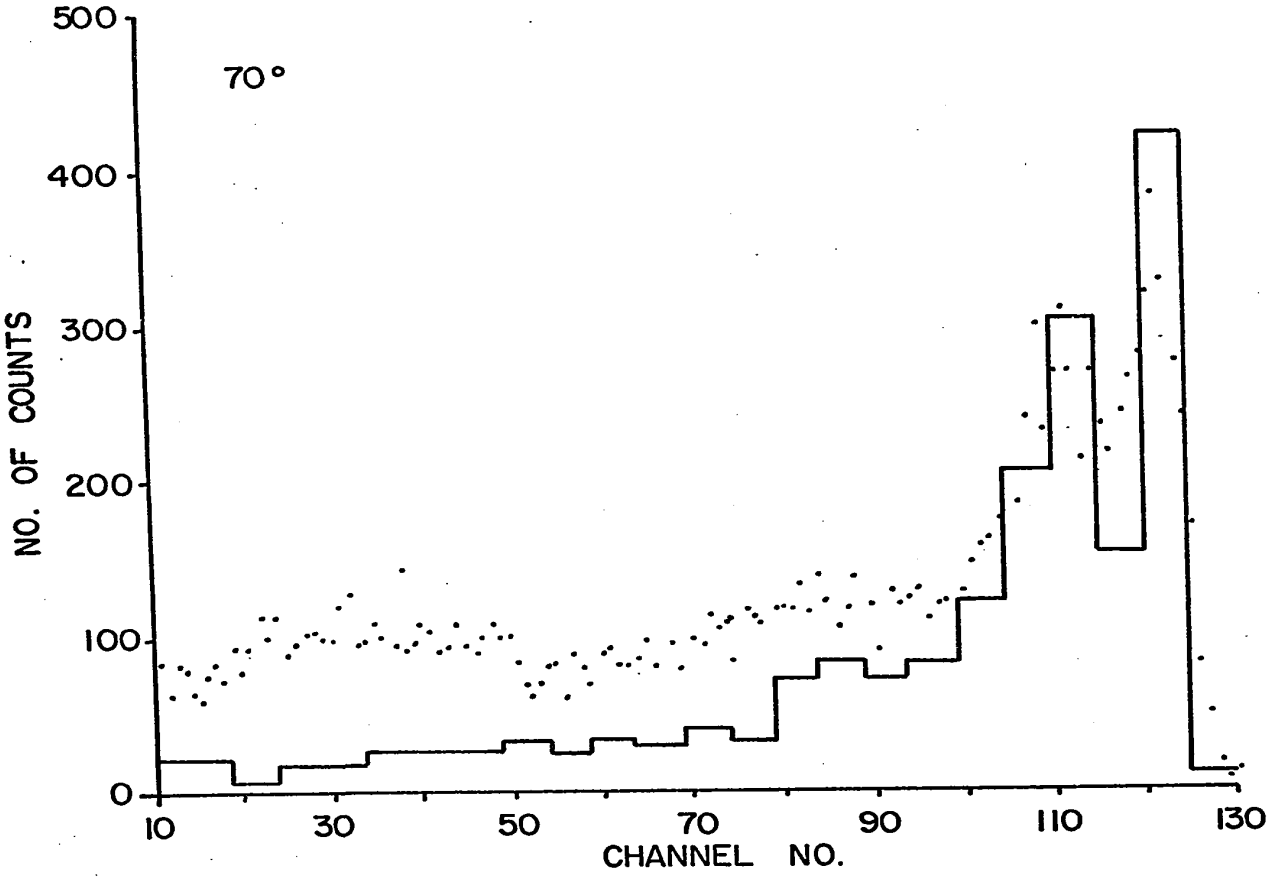

FIG. 13 COMPARISON OF TIME OF FLIGHT SPECTRA

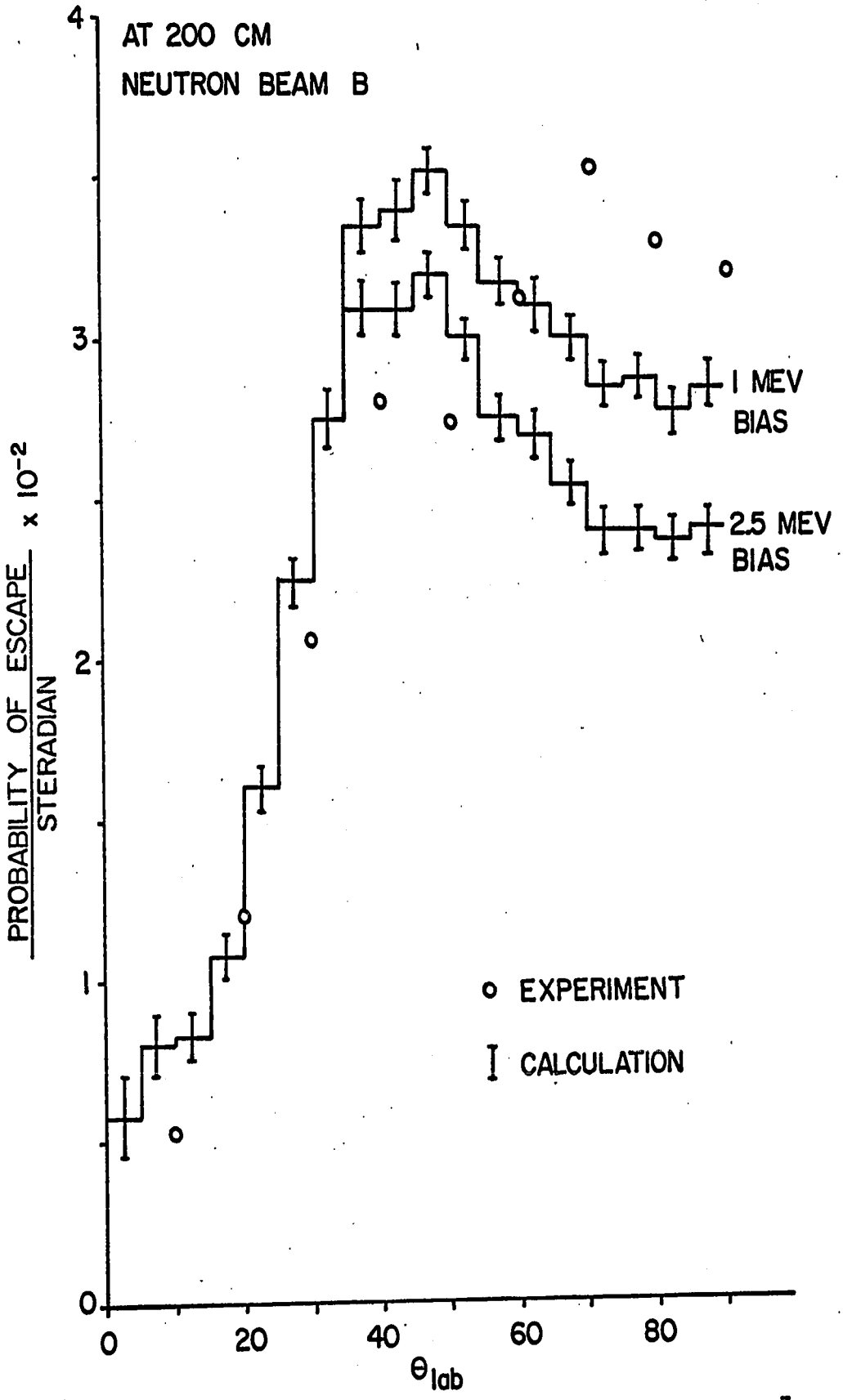

FIG. 14 ANGULAR DISTRIBUTION FOR 37 x 37 x 74 CM^3

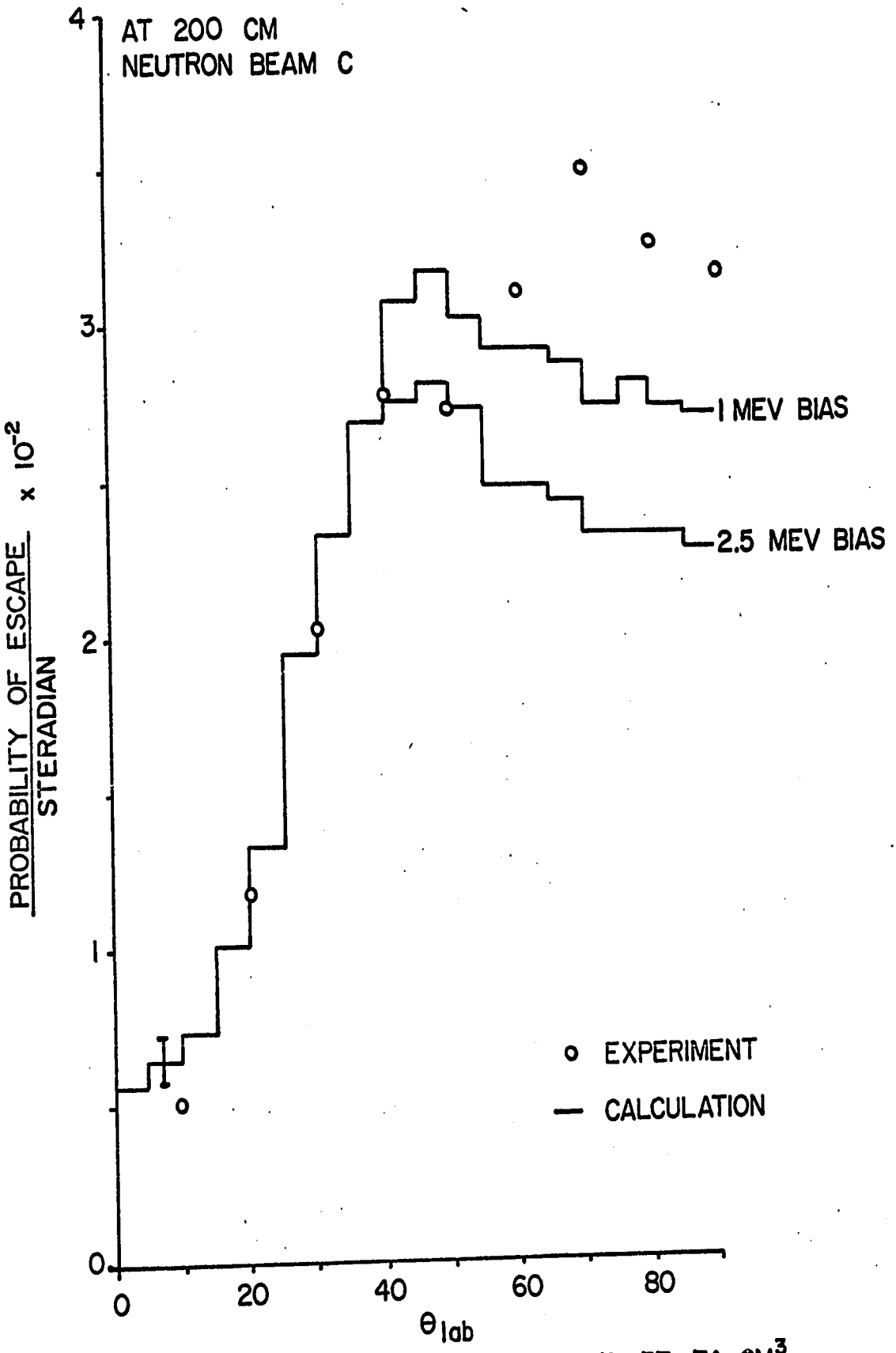

FIG. 15 ANGULAR DISTRIBUTION FOR 37 x 37 x 74 CM^3

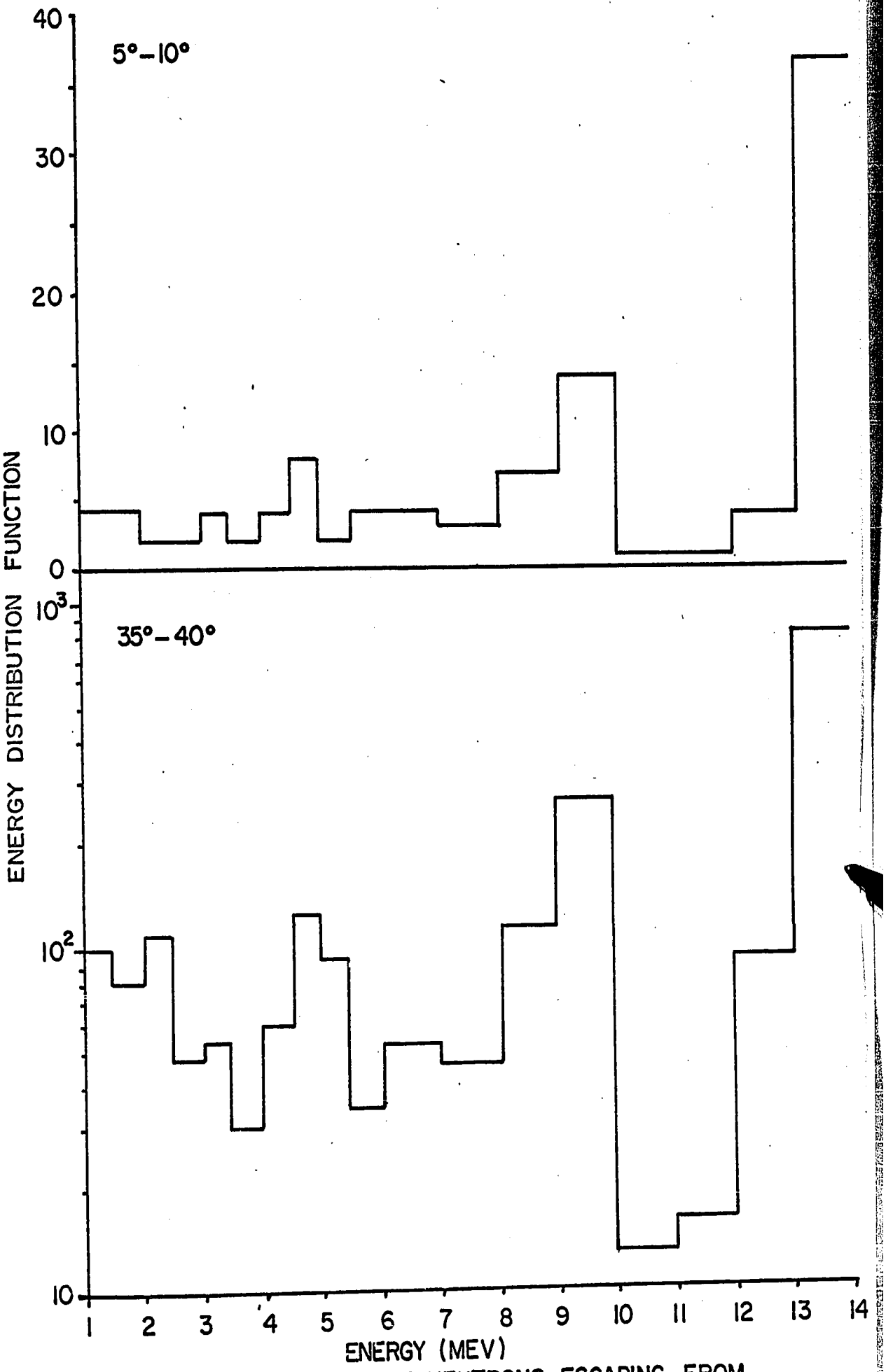

FIG. 16 ENERGY SPECTRA OF NEUTRONS ESCAPING FROM $37 \times 37 \times 74$ CM^3 BLOCK

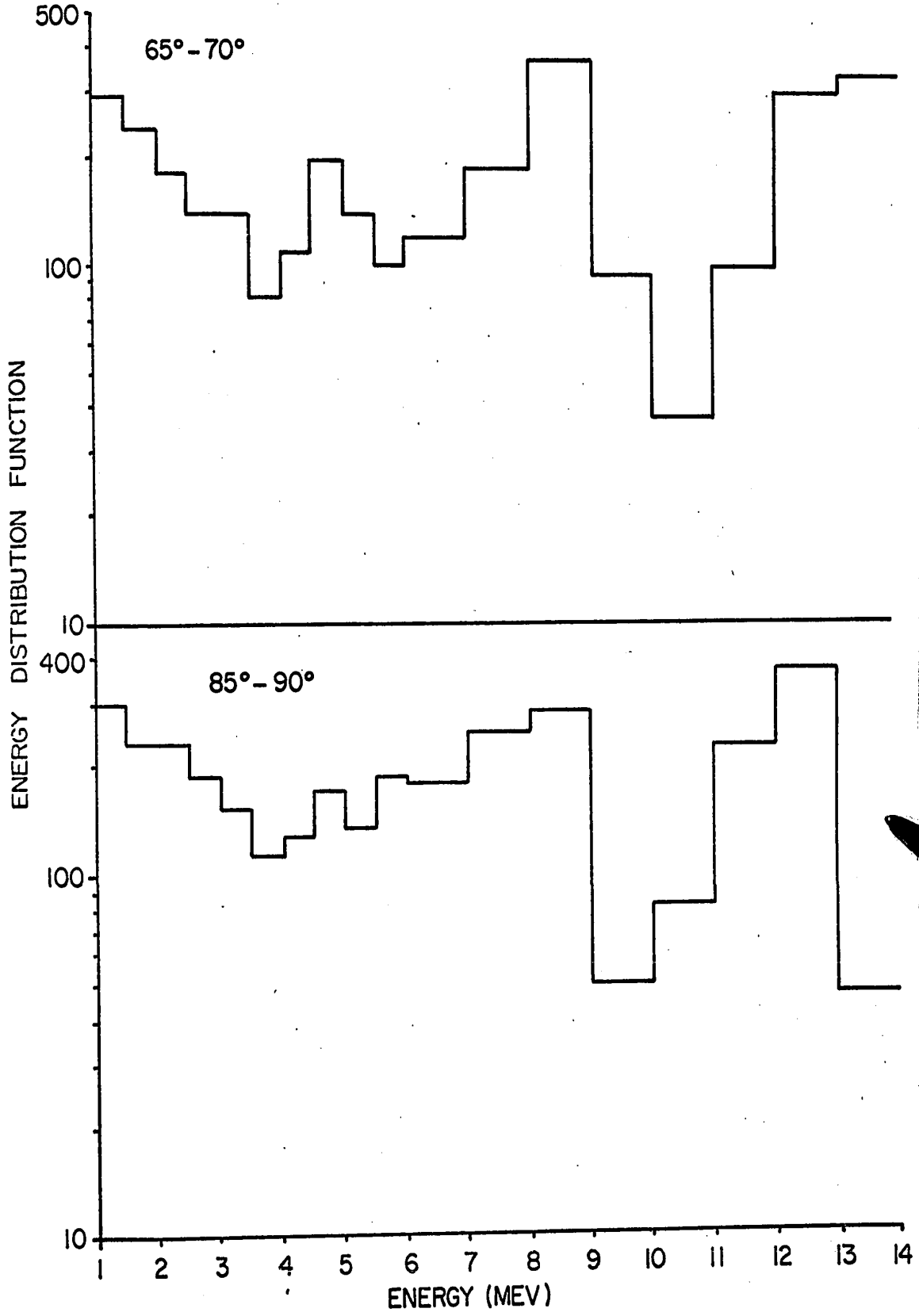

FIG. 17 ENERGY SPECTRA OF NEUTRONS ESCAPING FROM $37 \times 37 \times 74$ CM^3 BLOCK

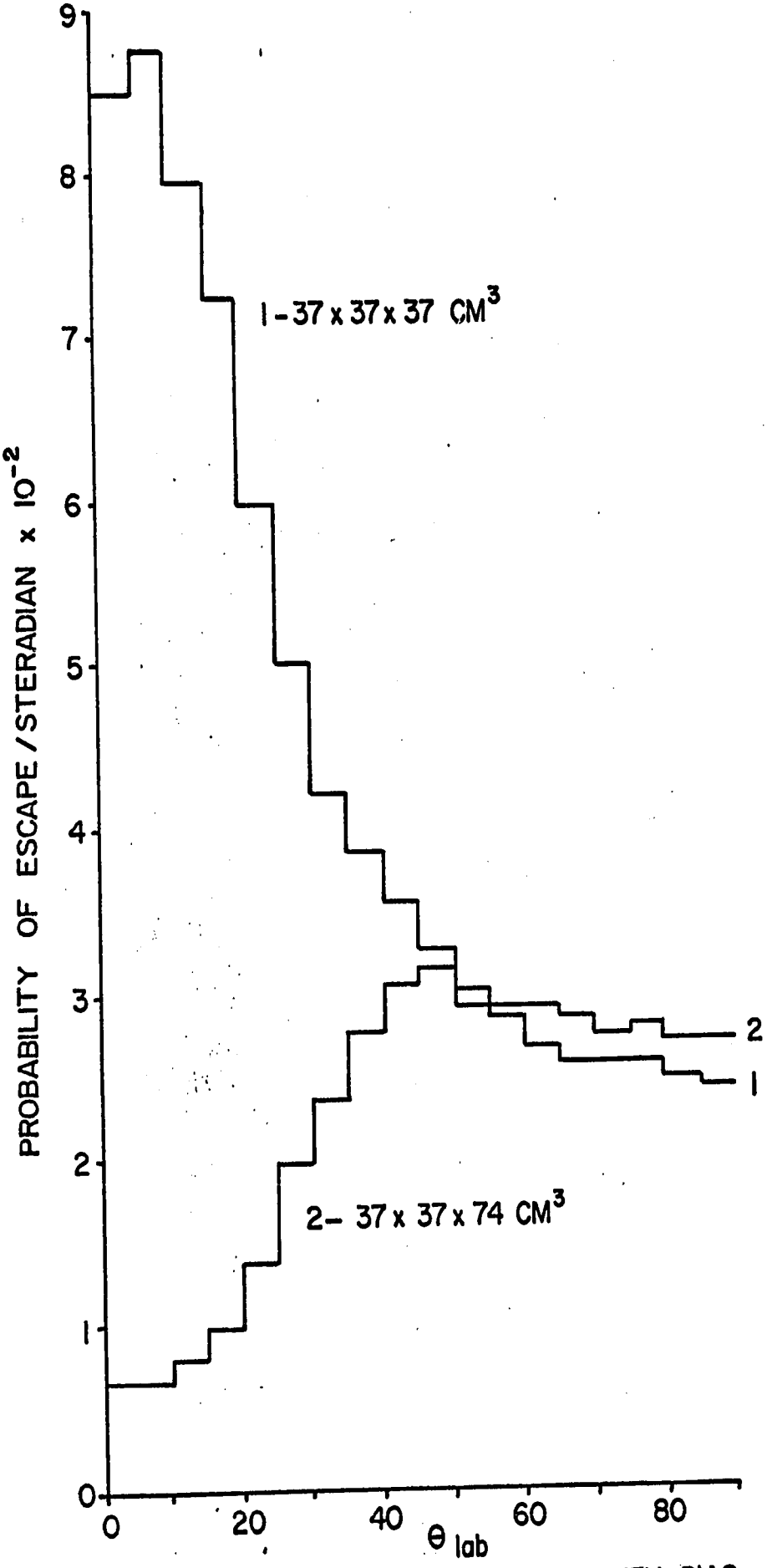

FIG. 18 ANGULAR DISTRIBUTION AT 1 MEV. BIAS

8. CONCLUSION

The aim of this project has been achieved: the calculated angular and time distributions agree basically with the experimental results. As it will require a few runs on the computer to determine which parameters must be changed to obtain a better agreement, and as essentially nothing new will be learned, one should go ahead with the calculations and experiments for concrete blocks.

To do a rigorous Monte Carlo calculation for concrete, it is necessary to know the following data for each nucleus found in concrete: the density of nuclei, the total and absorption cross-sections, and the differential elastic and inelastic cross-sections--all as a function of neutron energy. Unfortunately, only the density of nuclei and the total cross-section will be readily available. Therefore, the calculations must be done in the following manner. From the density of the various nuclei, n_i, and the total cross-sections, $\sigma_i(E)$, we can calculate the mean free path, $\lambda(E)$, for neutrons of energy E, $\lambda(E) = \left[\sum_i n_i \sigma_i(E)\right]^{-1}$; hence we shall be able to calculate the distance traversed by a neutron between

collisions. The elastic and inelastic angular distributions for 14 Mev neutrons can be measured in the laboratory using a 2-cm. thick concrete target. By examining the excited states of the nuclei, we should be able to put a limit beyond which no inelastic scattering occurs. The scattering at low energies (1 or 2 Mev) should be isotropic; therefore, from the total cross-section we can calculate the differential cross-section. Hence for neutrons of intermediate energy we shall use differential cross-sections obtained by a linear interpolation between the high and low energy differential cross-sections. By integrating these angular distributions, we shall determine the total elastic and inelastic cross-sections; by subtracting these from the total cross-sections, we shall obtain the absorption cross-sections. Thus, the calculations will be done as though concrete were monoisotopic.

The following changes in the computer program are recommended. The time required to do the calculations on the computer can be decreased by using a method known as "weighting" the neutrons. In the present program many neutrons are lost due to absorption. To avoid this we should attach a "weight" of one to neutrons as they enter the scattering material. Instead of "gambling" to determine whether the neutron was elastically or inelastically scattered, or absorbed, each time

a collision occurs, we reduce the weight, W, of the neutron by W_p, where p is the probability of absorption for that particular neutron; and then we gamble to determine whether the neutron was elastically or inelastically scattered. When escaping neutrons are classified, we must keep track of the number escaping in a particular direction and their "weight." The first counter gives the statistical error; the second gives the angular distribution. As there is sufficient storage space in the IBM 7090 computer there is no need to feed the angular distributions in the form of polynomials. Instead, we can feed a table which gives the value of the differential cross-section relative to the maximum value of the differential cross-section, i.e. $\frac{d\sigma(\theta)}{d\Omega}/\max\left(\frac{d\sigma(\theta)}{d\Omega}\right)$, for angles from 0° to 180° in 5° intervals. This latter method describes the differential cross-sections more accurately than polynomials obtained by a least square fit, especially at large angles.

APPENDIX A

CROSS SECTIONS AND ANGULAR DISTRIBUTIONS USED FOR CALCULATIONS*

TABLE I

(a) Elastic Scattering
14 Mev data used for the range 12 to 14 Mev--ref. 4
9.5 Mev data used for the range 9 to 12 Mev--ref. 5
7.0 Mev data used for the range 6 to 9 Mev--ref. 6
4.0 Mev data used for the range 3.6 to 4.5 Mev--ref. 8
3.0 Mev data used for the range 3 to 3.1 Mev--ref. 8
2.9 Mev data used for the range 2.9 to 3 Mev--ref. 8
2.5 Mev data used for the range 2.25 to 2.9 Mev--ref. 8
1 Mev data used for the range 1 to 2.25 Mev--ref. 8
(b) Inelastic Scattering
14 Mev data used for the range 12 to 14 Mev--ref. 4
9.5 Mev data used for the range 9 to 12 Mev--ref. 5
6.5 Mev data used for the range 4.8 to 9 Mev--ref. 9

*The data used were taken from Anderson et al.,[4] Burchan et al.,[5] Beyster et al.,[6] Hill,[7] Wills et al.,[8] and Brown and Lamarche,[9] as listed in Table I.

Reasonable extrapolations were used for the gaps where experimental data were not available.

APPENDIX B

ANGULAR DISTRIBUTION COEFFICIENTS

The polynomials describing the differential cross-section, normalized to the maximum value of the differential cross-section, are of the form $\sum_{n=0}^{6} a_n x^n$, where x is the cosine of the laboratory scattering angle.

Type of Scattering	Energy range (Mev)	a_0	a_1	a_2	a_3	a_4	a_5	a_6
Elastic	12-14	0.043	-0.004	-0.144	-0.174	0.228	0.670	0.381
	9-12	0.160	0	0.884	0.135	2.353	0.347	-1.111
	6-9	0.158	-0.017	0.532	0.503	-0.176	0	0
	4.5-6	0.127	0.098	0	-0.520	-0.668	0.905	1.058
	3.6-4.5	0.109	0	0	-0.326	1.256	0.495	-0.534
	3.1-3.6	0.007	0	1.200	-0.032	-0.602	0.057	0.370
	3-3.1	1	0	0	0	0	0	0
	2.9-3.0	0.028	0	+1.194	-0.081	-1.294	0.089	1.064
	2.25-2.9	0.177	+0.008	+1.857	+0.231	-3.351	-0.332	2.224
	1-2.25	1	0	0	0	0	0	0
Inelastic	12-14	0.131	0	0	0.276	0.106	0.166	0.321
	9-12	0.317	0.093	0	-0.530	2.176	0.691	-1.747
	4.8-9	1	0	0	0	0	0	0

BIBLIOGRAPHY

(1) Marshak, R. E., Revs. Modern Phys. 19, 185 (1947).

(2) Cashwell, C. D. and Everett, R. J., Random Walk Problems, Pergamon Press (1959).

(3) Owen, R. B., Proc. of the International Symposium on nuclear electronics organized by the French Society of Radioelectricians 1, 27 (1959).

(4) Anderson, J. D., et al., Phys. Rev. 111, 572 (1958).

(5) Burcham, W. E., et al., Phys. Rev. 92, 1266 (1953).

(6) Beyster, J. R., et al., Phys. Rev. 104, 1319 (1956).

(7) Hill, R. W., Phys. Rev. 109, 2105 (1958).

(8) Wills, J. E., et al., Phys. Rev. 109, 891 (1958).

(9) Brown, C. P. and Lamarche, J. R., Phys. Rev. 104, 1099 (1956).

(10) Reithmeier, J., et al., Nuclear Inst. & Methods 10, 240 (1961).

VITAE

NAME Corrado Glavina

BORN Rovigno d'Istria, Italy, 1940

EDUCATED:

University: Sir George Williams University

1956-1961

Course: Physics

Degree: B.Sc., 1960